



HAL
open science

Potential of polysaccharides for food packaging applications. Part 1/2: An experimental review of the functional properties of polysaccharide coatings

María Ureña, Thị Thanh-Trúc Phùng, Massimiliano Gerometta, Luciana de Siqueira Oliveira, Julie Chanut, Sandra Domenek, Patrice Dole, Gaele Roudaut, Aurélie Lagorce, Thomas Karbowiak

► To cite this version:

María Ureña, Thị Thanh-Trúc Phùng, Massimiliano Gerometta, Luciana de Siqueira Oliveira, Julie Chanut, et al.. Potential of polysaccharides for food packaging applications. Part 1/2: An experimental review of the functional properties of polysaccharide coatings. *Food Hydrocolloids*, 2023, 144, pp.article 108955. 10.1016/j.foodhyd.2023.108955 . hal-04158074

HAL Id: hal-04158074

<https://institut-agro-dijon.hal.science/hal-04158074v1>

Submitted on 26 Aug 2024

HAL is a multi-disciplinary open access archive for the deposit and dissemination of scientific research documents, whether they are published or not. The documents may come from teaching and research institutions in France or abroad, or from public or private research centers.

L'archive ouverte pluridisciplinaire **HAL**, est destinée au dépôt et à la diffusion de documents scientifiques de niveau recherche, publiés ou non, émanant des établissements d'enseignement et de recherche français ou étrangers, des laboratoires publics ou privés.

36 (oxygen permeance $> 10^{-12} \text{ mol.m}^{-2}.\text{s}^{-1}.\text{Pa}^{-1}$). This opens on interesting perspectives for the
37 use of polysaccharides as coating materials for high oxygen barrier packaging.

38 **Keywords:** polysaccharides, biopolymer film, multilayer packaging, paper-based packaging,
39 coatings.

40 **1. Introduction**

41 Conventional petroleum-based plastics, such as polyethylene terephthalate (PET), polyamide
42 (PA), high-density polyethylene (HDPE), linear low-density polyethylene (LLDPE), polypro-
43 pylene (PP), and ethylene vinyl alcohol (EVOH), still dominate the food packaging sector
44 (Stoica, Antohi, Zlati & Stoica, 2020). Although they offer numerous advantages, they also
45 represent a waste to manage and a potential pollution when the collection system fails. The
46 main issue with their use for food packaging remains the post-consumer waste, where pack-
47 aging is by far the most significant contributor of plastic waste worldwide. Packaging repre-
48 sents 47 % of the total plastic waste, which corresponded to 141 million tons of plastic waste
49 in 2015 (United Nations Environment Programme, 2018). According to Parker (2019), half of
50 all plastics ever manufactured have been produced in the last 15 years. The production has
51 increased from 2.3 million tons in 1950 to 448 million tons in 2015 and is expected to double
52 by 2050. Only 14 % of all plastic waste ever produced has been recycled, 14 % has been in-
53 cinerated, and the rest (72 %) has been accumulated in landfills and water bodies around the
54 world (United Nations Environment Program, 2018).

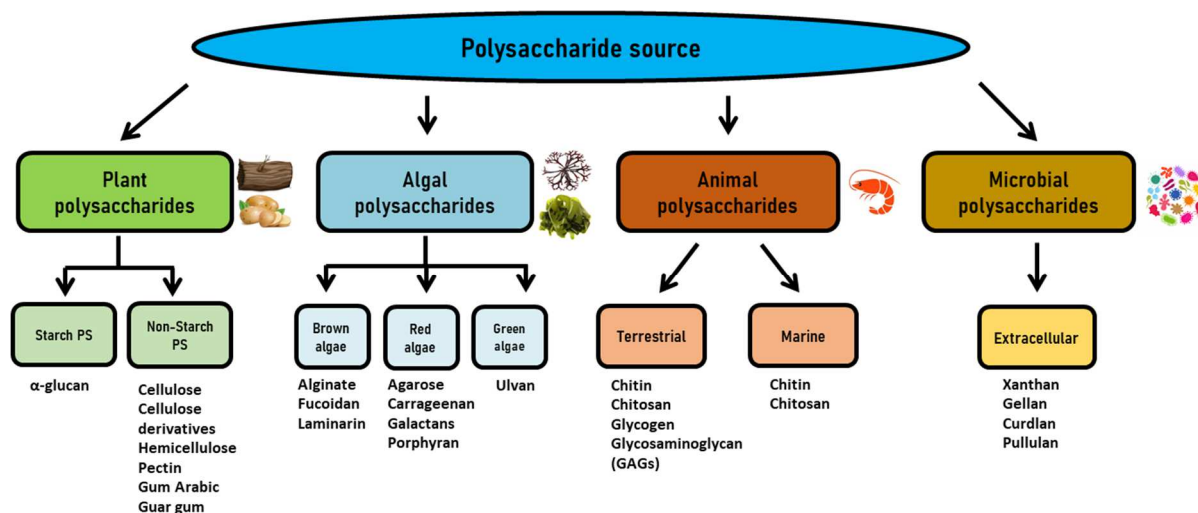
55 For this reason, different strategies have recently been implemented around the world. In Eu-
56 rope, the "European Strategy for Plastics in a Circular Economy", aims at reducing the de-
57 pendence on fuel-based raw materials, increasing the recyclability of plastics and reducing
58 the leakage of plastics into the environment (European Parliament and Council, 2018). This
59 strategy targeted the end of single-use plastics by 2040. As a consequence, one of the strate-
60 gies consists in substituting conventional plastics by paper-based materials. Several food
61 product brands worldwide are switching from traditional plastic to paper-based packaging in
62 order to shift to recyclable materials and to decrease the impact of plastics on the environ-
63 ment. However, even though paper is recyclable and even compostable under certain condi-
64 tions (Venelampi, Weber, Rönkkö & Itävaara, 2003), it has significant drawbacks such as
65 high porosity and, therefore, poor barrier properties towards water vapor and oxygen
66 (Deshwal, Panjagari & Alam, 2019). Thus, to lessen these disadvantages, paper-based pack-
67 aging is usually coated with conventional fossil-based polymers like polypropylene (PP) and
68 polyethylene (PE). However, this practice compromises its recyclability and increases the
69 carbon footprint of the packed food.

70 Biopolymers, especially those derived from renewable organic resources, such as polysaccha-
71 rides and proteins, seem to be a promising solution to replace conventional polymers in spe-

72 cific applications (Tardy et al., 2022). Most films made from proteins and polysaccharides
 73 generally exhibit excellent barriers to gases, aromas and lipids and have acceptable mechani-
 74 cal strength (Nechita & Roman, 2020). However, these biopolymers show a very high sensi-
 75 tivity to water due to their hydrophilic nature (Stoica et al., 2020), which is the main limita-
 76 tion when considering their use for food packaging applications.

77 Many investigations were based on the exclusive use of proteins for packaging applications
 78 (Kchaou, Jridi, Benbettaieb, Debeaufort & Nasri, 2020; Salem et al., 2021; Xu et al., 2022).
 79 However, proteins generally find higher value-added applications as food or feed ingredients.
 80 Conversely, polysaccharides are the most abundant natural polymers (Guo, Liu & Cui, 2021).
 81 Their extraction and chemical modification are relatively easy-performing, thus making them
 82 readily available on the market at a relatively lower price. Therefore, polysaccharides might
 83 be considered the most suitable candidates for food packaging applications, such as coatings
 84 or self-standing films, and for the design of new food packaging materials, such as paper-
 85 based and multilayer packaging.

86 Polysaccharides can be classified according to their source, dividing them into four catego-
 87 ries, namely plant, algal, animal, and microbial polysaccharides (Guo et al., 2021; Yadav &
 88 Karthikeyan, 2019). Each category can be further divided into subcategories depending on
 89 the environment from which the polysaccharides are extracted (Fig. 1).



90 Fig 1. Classification of polysaccharides according to their source. (Adapted from Guo et al., 2021 and Yadav & Karthikeyan,
 91 2019).

92 The molecular structures of polysaccharides are quite complex due to many variables, includ-
 93 ing the composition of the monosaccharides, the stereochemistry of glycosidic bonds, the

94 degree of branching, branch positions, the presence of functional groups and the molecular
95 weight distribution, amongst others (Edens, 2005). Based on these premises, a study of sever-
96 al polysaccharides with different molecular structures is strictly sought after to provide a mul-
97 ti-criteria overview of their potential applicability in the food packaging sector.

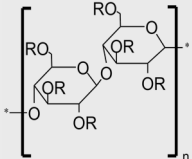
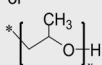
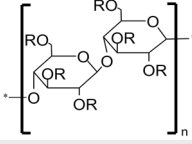
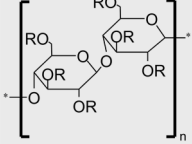
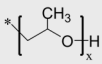
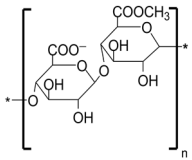
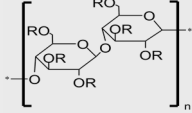
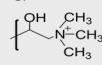
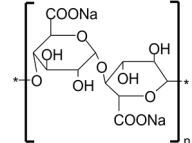
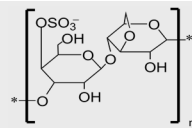
98 Although extensive information on the performance of different polysaccharide films for
99 food packaging applications is already available, it remains challenging to compare results
100 from the literature due to the lack of compatibility of results and standardization of methods.
101 Accordingly, the objective of this study was to offer an extensive overview of the main phys-
102 icochemical properties of nine different polysaccharides under standardized conditions. Their
103 properties were evaluated as film-forming solutions for viscosity and surface tension and as
104 self-standing films (produced by the solvent casting method) for the barrier, mechanical and
105 optical properties.

106 **2. Materials and methods**

107 **2.1. Materials**

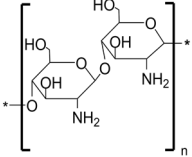
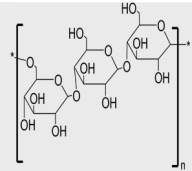
108 Nine different polysaccharides from different natural sources, highly studied for their poten-
109 tial food packaging applications, were selected (**Table 1**). The plasticizer chosen for all the
110 polysaccharides was glycerol ($\geq 99.5\%$, Fisher Scientific, Strasbourg, France). Lactic acid
111 (90 %, ProLABO, Paris, France) was additionally used only for the solubilization of chitosan
112 as reported in the next section.

113 Table 1. Main physicochemical characteristics of the polysaccharides selected in this work as film-forming materials.

Organ	Polysaccharide	Abbreviation	Structure	Specification	Moisture content (%) ^a	Ash content (%) ^b	Source	Supplier n° CAS	Purity (%)	E _{coh} ^c (kJ/mol)	δ _c ^d (MPa ^{1/2})
Plant	Hydroxypropyl Methyl Cellulose	HPMC	 R = H or CH ₃ or 	Uncharged, soluble in water at T < 45 °C, methyl = 28-30 % and hydroxypropyl = 7-12 %	5.92 (±0.14)	0.18 (±0.01)	Semi-synthetic cellulose derivative	Sigma Aldrich, (Saint-Quentin-Fallavier, France) CAS: 9004-65-3	≥ 93.5	85.2	50.2
Plant	Methyl Cellulose	MC	 R = H or CH ₃	Uncharged, soluble in water at T < 40-55 °C	6.46 (±0.21)	0.47 (±0.01)	Semi-synthetic cellulose derivative	(Louis François, Croissy-Beaubourg, France) CAS: 9004-67-5	≥ 88.5	54.1 - 71.4	23.9 - 38.7
Plant	Hydroxypropyl Cellulose	HPC	 R = H or 	Uncharged, soluble in water at T < 45 °C	16.26 (±0.14)	0.17 (±0.02)	Semi-synthetic cellulose derivative	Sigma Aldrich CAS: 9004-64-2	≥ 95	106.1 - 163.6	32.8 - 40.3
Plant	Low-Methoxyl Pectin	LMP		Anionic Galacturonic acid ≥ 74 %, pKa = 3.5	11.15 (±0.18)	8.86 (±0.68)	Pectin from citrus peels	Sigma Aldrich CAS: 9000-69-5	≥ 90	92.6	49.2
Plant	Cationic Starch	CS	 R = H or 	Cationic degree of substitution: 1.4-1.6 %	13.94 (±0.10)	3.36 (±0.13)	Potato starch	Cargill (Hau-bourdin, France) CAS: 56780-58-6	N.S	N.S	N.S
Algae	Sodium Alginate	SA		Anionic pKa = 3.2	14.51 (±0.24)	31.34 (±1.63)	Brown seaweed <i>Phaeophyceae</i>	Sigma Aldrich CAS: 9005-38-3	≥ 84.5	95.1	46.1
Algae	Kappa-Carrageenan	KC		Anionic pKa = 4.9, solubility = 5 g/L in water at T > 80 °C	11.03 (±0.27)	20.93 (±0.07)	Red seaweed	Sigma Aldrich CAS: 11114-20-8	≥ 88	N.S	N.S

114

115 Table 1 (continued)

Origin	Polysaccharide	Abbreviation	Structure	Specification	Moisture content (%) ^a	Ash content (%) ^b	Source	Supplier n° CAS	Purity (%)	E _{coh} ^c (kJ/mol)	δ _t ^d (MPa ^{1/2})
Animal	Chitosan	CHI		Cationic 75-85 % deacetylated, pKa = 6.5	8.71 (±0.02)	0.58 (±0.07)	Deacetylated product of chitin	Sigma Aldrich CAS: 9012-76-4	N.S	96.8 - 113.2	42.8 - 45.6
Microbial	Pullulan	PL		Uncharged	11.25 (±0.13)	0.27 (±0.01)	Polymer of maltotriose produced from starch by the fungus <i>Aureobasidium pullulans</i>	ATP Chemical, (Shanghai, China) CAS: 9057-02-7	≥ 95.9	102.2	53.1

116 ^aMoisture content was determined by heating the samples at 103 °C until constant mass for samples previously stored at 25 °C and 50 % relative humidity (RH). ^bAsh content was determined by
 117 furnacing the samples at 500 °C for 10 h. Values are reported as mean ± standard deviation. Number of replicates (n) = 3. Other data were provided by suppliers. **N.S:** Not Specified. ^cCohesive
 118 energy density (E_{coh}) of the polysaccharides was calculated according to the group contribution method based on Fedors (Krevelen & Nijenhuis, 2009). ^dOverall solubility parameter (δ_t) of the
 119 polysaccharides was calculated according to the group contribution method based on Van Krevelen (Hansen, 2007).

120 **2.2. Preparation of film-forming solutions**

121 All the film-forming solutions were prepared following the same procedure. Only slight mod-
122 ifications related to mixing time, temperature and air bubbles removal method were applied
123 depending on the properties of each polysaccharide, as described below. For the preparation
124 of the film-forming solutions, 2 % (w/w) of each polysaccharide was slowly dispersed in 1
125 liter of distilled water together with glycerol at different percentages (0, 10, 20, or 30 %
126 (w/w) based on a dry basis). For the cellulose derivatives (HPMC, MC, and HPC), SA and PL
127 solutions, the polysaccharides were dispersed in distilled water at 25 °C and stirred at 500
128 rpm until complete dissolution (around 1 hour). The solutions were then treated using an ul-
129 trasonic bath (Branson 3510; Milford, Connecticut, USA) with a frequency of 40 Hz and a
130 power of 130 W for 1 hour to remove air bubbles. CHI was dispersed in distilled water con-
131 taining 1 % (v/v) lactic acid at 25 °C and stirred at 500 rpm until complete dissolution
132 (around 1 hour). No treatment was required for the removal of air bubbles in that case. KC,
133 CS and LMP were dissolved in distilled water at 90 °C for the first two and 70 °C for the last
134 one and stirred at 500 rpm until complete dissolution (around 1 hour). The solutions were
135 then treated under vacuum to remove air bubbles.

136 **2.3. Films formation**

137 The solutions previously prepared (according to the protocol described in section 2.2.1) were
138 casted in square polystyrene (PS) Petri dishes (12 x 12 cm²) to form the films. Then, they
139 were dried at 25 °C and 50 % RH for 48 h. Calibration curves were previously established for
140 each film-forming solution to determine the exact amount of solution required to be poured
141 into the Petri dish in order to achieve 50±5 µm thick film in all cases (data not shown). The
142 thickness was controlled in at least five different positions using a micrometer Thickness
143 Gauge FD-100 with a resolution of 0.001mm (Hans Schmidt & Co GmbH; D-84478,
144 Waldkraiburg, Germany).

145 **2.4. Film-forming solutions characterization**

146 **2.4.1. Rheological properties**

147 The rheological properties of the solutions (shear stress τ and apparent viscosity μ_{ap}) were
148 determined using a rotational rheometer (HAAKE™ RotoVisco™ 1; Thermo Fisher Scien-
149 tific, Boston, USA) at 25±1 °C for all polysaccharide solutions, except for Kappa-
150 Carrageenan (KC), which was measured at 70±1 °C. A Z34DIN sensor with a rotor No 222-
151 1499 (radius = 17.00 mm, length 51 mm, clearance to bottom 7.2 mm) and a cup No 222-

1498 (radius = 18.44 mm), were used for the analysis. Measurements were done in triplicate
 153 for the polysaccharide solutions without glycerol. The rheological properties were recorded at
 154 shear rates from 0.5 s^{-1} to 200 s^{-1} .

155 **2.4.1.1. Shear stress**

156 The experimental data of the polysaccharide flow curves (shear stress τ according to shear
 157 rate $\dot{\gamma}$) were analyzed using the Ostwald de Waele model fitting (**Eq. 1**):

$$158 \quad \tau = \kappa \dot{\gamma}^n \quad (1)$$

159 where τ is the shear stress (Pa), $\dot{\gamma}$ is the shear rate (s^{-1}), κ is the consistency index ($Pa \cdot s^n$)
 160 and n is the flow behavior index (dimensionless).

161 **2.4.1.2. Apparent viscosity**

162 The apparent viscosity (μ_{ap}) of the polysaccharide solutions was extrapolated using κ and n
 163 constants previously calculated to predict the apparent viscosity of the solutions at 1000 s^{-1} .
 164 The values of apparent viscosity at 10 s^{-1} and 1000 s^{-1} were chosen as targeted values to
 165 compare the different polysaccharide solutions and their application as coatings.

166 **2.4.2. Surface tension**

167 The total surface tension (σ_L) of the solutions and their polar (σ_L^p) and dispersive (σ_L^d) com-
 168 ponents were determined at $25 \pm 1 \text{ }^\circ\text{C}$ using a Krüss K100 tensiometer (Krüss GmbH, Ham-
 169 burg, Germany). At least 5 repetitions were made for the polysaccharide solution without
 170 glycerol. The total surface tension (σ_L) was measured using the Wilhelmy method with a plat-
 171 inum plate and was furtherly calculated according to **Eq. 3**:

$$172 \quad \sigma_L = \frac{F}{L \cdot \cos\theta} \quad (3)$$

173 where σ_L is the total surface tension ($mN \cdot m^{-1}$), F is the force measured (mN), L is the wetted
 174 length (m), and θ is the angle formed between the plate and the liquid, which corresponds to
 175 0° in the case of the platinum plate.

176 **2.4.2.1. Dispersive and polar components**

177 The dispersive component of the surface tension was determined by the contact angle meas-
 178 urement using a polytetrafluoroethylene (PTFE) plate and it was calculated using the Owens
 179 and Wendt equation (**Eq. 4**):

$$180 \quad \frac{\sigma_L (\cos\theta + 1)}{2\sqrt{\sigma_L^d}} = \frac{\sqrt{\sigma_S^p} \cdot \sqrt{\sigma_L^p}}{\sqrt{\sigma_L^d}} + \sqrt{\sigma_S^d} \quad (4)$$

181 where σ_L is the total surface tension of the liquid ($\text{mN}\cdot\text{m}^{-1}$) determined by the Wilhelmy
 182 method, θ is the contact angle between the solid (PTFE plate) and the liquid. σ_L^d is the disper-
 183 sive part of the liquid ($\text{mN}\cdot\text{m}^{-1}$), σ_L^p is the polar part of the liquid ($\text{mN}\cdot\text{m}^{-1}$). σ_S^d is the disper-
 184 sive part of the solid and σ_S^p is the polar part of the solid ($\sigma_S^d = 18$ ($\text{mN}\cdot\text{m}^{-1}$) and $\sigma_S^p = 0$
 185 ($\text{mN}\cdot\text{m}^{-1}$) in the case of PTFE plate).

186 By rearranging the above equation (4), the dispersive part of the solutions was then calculated
 187 as shown in **Eq. 5**:

$$188 \quad \sigma_L^d = \frac{\sigma_L^2(\cos\theta+1)^2}{4\cdot\sigma_S^d} \quad (5)$$

189 Ultimately, the polar part of the solutions was then calculated according to **Eq. 6**:

$$190 \quad \sigma_L^p = \sigma_L - \sigma_L^d \quad (6)$$

191 **2.4.2.2. Wetting envelope**

192 The wetting envelope analysis was performed to predict the contact angle of polysaccharide
 193 solutions on a solid surface. Kraft paper was chosen in the present case. The polar and disper-
 194 sive components of the polysaccharide solutions were entered into a coordinate system.
 195 Hence, the wetting parameter R was obtained from a geometrical transformation using **Eq. 7**,
 196 with $\sigma_L^p = R \cdot \sin\varphi$ the polar component and $\sigma_L^d = R \cdot \cos\varphi$ the dispersive component. R and φ
 197 are the auxiliary polar coordinates to calculate the wetting envelope.

$$198 \quad R = \sqrt{(\sigma_L^d)^2 + (\sigma_L^p)^2} \quad (7)$$

199 R is also related to the dispersive and polar components of the surface tension of the solid by
 200 the relation (**Eq. 8**):

$$201 \quad R(\varphi) = \left(\frac{2}{1+\cos\theta} \frac{\sqrt{\cos\varphi \cdot \sigma_S^d + \sin\varphi \cdot \sigma_S^p}}{\cos\varphi + \sin\varphi} \right)^2, \text{ for } 0^\circ \leq \varphi \leq 90^\circ \quad (8)$$

202 In this equation, R can be calculated for different angles φ between 0° and 90° , to form a wet-
 203 ting envelope that describes the polar and dispersive surface tension for theoretical wetting of
 204 the surface with different contact angles θ . The wetting envelopes corresponding to a contact
 205 angle of 0° , 20° , 40° , 60° , 80° and 100° were plotted.

2.5. Films characterization

2.5.1. Moisture sorption isotherms

Rectangular specimens of the films (dimensions 2 x 1 cm²) without and with 30 % glycerol were equilibrated in triplicate under various relative humidity environments in air-tight containers. To that purpose, P₂O₅, or various saturated salt solutions (LiCl, KC₂H₃O₂, MgCl₂, K₂CO₃, NaBr, SrCl₂, KCl) were used at 25 °C, in order to set 0 %, 11.1 %, 23.1 %, 33 %, 46 %, 58.7 %, 72.5 % and 85.1 % RH, respectively. Equilibrium was considered to be achieved when the weight change did not exceed 0.05 % (wet basis) over one week. After equilibration, the samples were weighed using an analytical balance with an accuracy of 0.1 mg (Sartorius Analytical balance - Sartorius Lab Instruments GmbH & Co. KG – Goettingen, Germany). Then, the dry weight was determined using an oven at 103 °C for 24 h. The moisture content of the films was calculated according to **Eq. 9**.

$$MC (\%) = \frac{m_w - m_d}{m_d} \times 100 \quad (9)$$

Where *MC* is the moisture content (*dry basis*), *m_w* is the wet weight (*g*), and *m_d* is the weight after drying (*g*).

2.5.2. Mechanical properties

The mechanical behavior of the polysaccharide films was assessed by uniaxial tensile tests under ambient conditions (T ≈ 25 °C, RH ≈ 50 %) using a texture analyzer (TA.HD plus; Stable Micro Systems Company, Godalming Surrey GU7 1YL, United Kingdom). The tests were carried out following the standard method ISO 527-3:2018 with some modifications (International Organization for Standardization, 2018). A 30 kg load cell was used, and tests were performed with a constant crosshead speed of 50 mm.min⁻¹. Six to nine rectangular specimens for each polysaccharide film condition (dimensions 7 x 2.5 cm²), previously equilibrated at 50 % RH and 25 °C in a climatic chamber model KBF 240 (Binder GmbH, Tuttlingen, Germany), were prepared with a precision cutter (JDC; Thwing Albert Instrument Company, West Berlin, NJ, USA). Young's modulus (*GPa*), tensile strength (*MPa*) and elongation at break (%) were determined from the corresponding stress-strain curves.

2.5.3. Barrier properties to oxygen

The permeance of the polysaccharide films to oxygen (*P_{O₂}*) was determined by the manometric method using a GTT permeameter (Brugger Feinmechanik GmbH, Munich, Germany) at 25 °C under three different relative humidity conditions (10 %, 50 % and 80 % RH). The system was outgassed under primary vacuum before testing. At time zero, one side of the film

238 was flushed with the gas (flow $\approx 27 \text{ cm}^3 \cdot \text{min}^{-1}$) and the increase in pressure on the other side
239 was recorded over time. The partial pressure differential was 1000 hPa. The experiments
240 were performed in triplicate

241 The permeance (expressed in $\text{mol} \cdot \text{m}^{-2} \cdot \text{s}^{-1} \cdot \text{Pa}^{-1}$) was determined from the steady-state of the
242 transfer according to **Eq. 10**:

$$243 \quad P = \frac{\Delta n}{A \cdot \Delta t \cdot \Delta p} \quad (10)$$

244 where P is permeance, Δn is the average molar quantity associated with the gas transfer
245 (mol), A is the surface area of the film (m^2), Δt is the time (s), Δp is the pressure difference
246 between the two sides of the film (Pa).

247 **2.5.4. Barrier properties to water vapor**

248 The permeance of the polysaccharide films to water vapor (P_{H_2O}) was determined using the
249 gravimetric method at 25 °C, according to the standard method ISO 2528:2017 with some
250 modifications (International Organization for Standardization, 2017). Two different relative
251 humidity conditions were used. These two conditions are referred to, in the present work, as
252 "semi-dry" condition (0 %-50 % RH) and "humid" condition (50 %-100 % RH). For the
253 semi-dry condition, silica gel was used inside the permeability cell (3.4 cm inner diameter) to
254 maintain the relative humidity close to 0 %. For the humid condition, distilled water was used
255 inside the permeability cell to maintain a relative humidity close to 100 %. For both condi-
256 tions, the permeability cells containing silica gel or distilled water with the polysaccharide
257 film fixed between two silicon O-rings at the top were placed in a climatic chamber at 50 %
258 RH and 25 °C. The cell weight was measured once a day using an analytical balance with an
259 accuracy of 0.1 mg model A200 FS1 (Sartorius Analytical balance; Sartorius Lab Instruments
260 GmbH & Co. KG – Goettingen, Germany). The permeance to water vapor was determined
261 from the steady-state of the transfer according to **Equation 10**. The partial pressure differen-
262 tial was 1584 Pa for both "semi-dry" and "humid" conditions. The analyses were performed
263 in quadruplicate.

264 **2.5.6. Barrier properties to light**

265 The UV/Visible transmission spectra of the polysaccharide films without glycerol were
266 measured using a UV-Visible spectrophotometer (SAFAS UVmc, Monaco). The rectangular
267 specimens (dimensions $5 \times 2.5 \text{ cm}^2$) were fixed so that the light beam could pass through the
268 film. Air was used as the blank. Transmittance spectra were recorded at wavelengths between

269 200 and 800 nm. UV screening ability of the films was given as the percentage of transmit-
270 tance at 280 nm and transparency as the percentage of transmittance at 550 nm. The values
271 obtained were divided by the exact thickness of the measured sample and multiplied by 50
272 μm for normalization purpose. Three specimens were analyzed for each film.

273 **2.6. Statistical analysis**

274 Data were expressed as the mean \pm standard deviation of at least three replicates. A signifi-
275 cant difference in the mean was tested using one-way ANOVA Tukey's test at the 95 % confi-
276 dence level ($p < 0.05$). Data were processed using MATLAB 2014, Orange Data Mining
277 3.28.0 and IBM SPSS Statistic 20.

278 **3. Results and Discussion**

279 **3.1. Properties of polysaccharide film-forming solutions for their use as coatings**

280 **3.1.1. Rheological properties of film-forming solutions**

281 The rheological properties of the polysaccharide solutions were measured at different shear
 282 rates, from 0 to 200 s⁻¹ at 25±1 °C (except for KC, which was measured at 70±1 °C due to
 283 the gelation of KC at ambient temperature). Shear stress as a function of the shear rate is dis-
 284 played in **Fig. 2A**. The experimental shear data were fitted by the Ostwald de Waele model,
 285 which generally applies to flow curves for hydrocolloids (Ma, Lin, Chen, Zhao & Zhang,
 286 2014). The model parameters for the different polysaccharide solutions are reported in **Table**
 287 **2**. All the solutions displayed a pseudo-plastic fluid's non-Newtonian behavior, characterized
 288 by a flow behavior index (*n*) lower than 1. Nevertheless, LMP, SA and PL solutions presented
 289 a flow behavior index (*n*) approaching a unitary value, indicating to be relatively close to
 290 Newtonian fluids, and thus showing a lower influence of shear rate on viscosity. The Ostwald
 291 de Waele model fitted well the flow curves experimental data (with R² > 0.99), except for PL
 292 (with R² < 0.72), indicating that in this case the model was not suitable.

293 **Table 2.** Ostwald de Waele model fitting parameters and apparent viscosity values determined at a shear rate of 10 s⁻¹ and
 294 extrapolated by modeling at 1000 s⁻¹ for the different polysaccharide solutions at 25 °C.

Polysaccharide	μ_{ap} (Pa.s) at 10 S ⁻¹	μ_{ap} (Pa.s) at 1000 S ⁻¹ (*)	Ostwald de Waele model fitting parameters			
			<i>K</i>	<i>n</i>	<i>R</i> ²	<i>SD</i>
HPMC	1.991±0.176	0.469±0.045	4.845	0.662	0.997	6.080
MC	2.341±0.273	0.441±0.038	6.177	0.619	0.996	7.720
HPC	0.224±0.019	0.102±0.003	0.392	0.806	0.998	0.780
LMP	0.097±0.032	0.082±0.002	0.114	0.953	0.999	0.400
CS	0.275±0.021	0.030±0.001	0.818	0.522	0.996	0.350
SA	0.095±0.005	0.091±0.006	0.149	0.929	0.999	0.190
+KC	0.235±0.065	0.109±0.002	0.490	0.784	0.998	4.410
CHI	2.110±0.119	0.400±0.012	5.285	0.627	0.997	5.520
PL	0.004±0.002	0.003±0.001	0.005	0.948	0.720	0.040

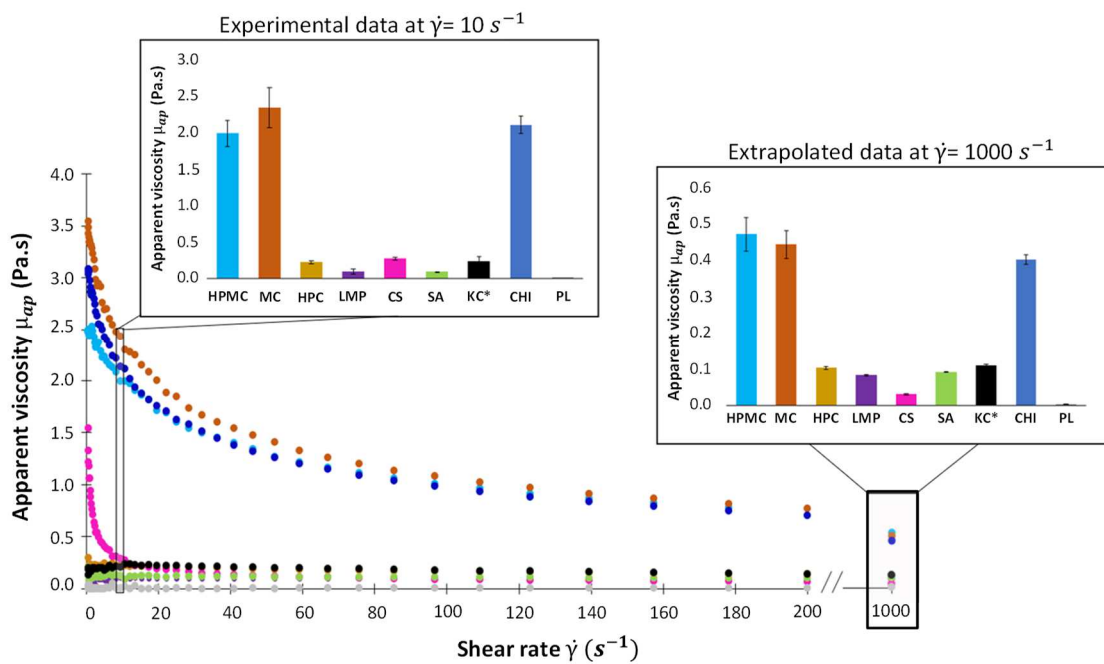
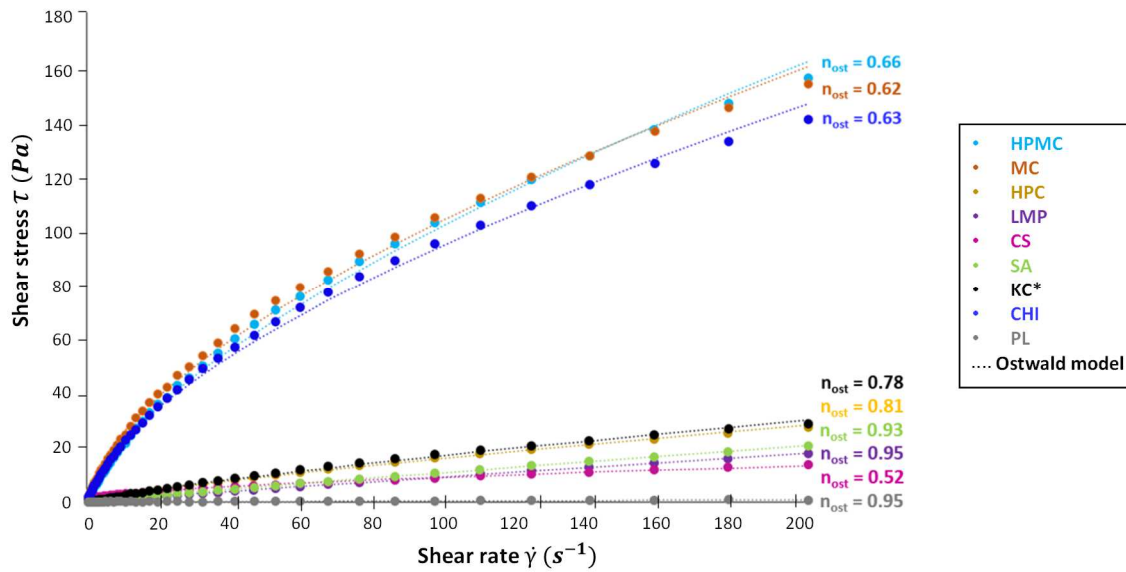
295 **HPMC:** Hydroxypropyl Methylcellulose. **MC:** Methyl Cellulose. **HPC:** Hydroxypropyl Cellulose. **LMP:** Low Methoxyl
 296 Pectin. **CS:** Cationic Starch. **SA:** Sodium Alginate. **KC:** Kappa-Carrageenan (+: Temperature of measurement 70(±1) °C).
 297 **CHI:** Chitosan. **PL:** Pullulan. Values of apparent viscosity at 10 s⁻¹ are reported as mean ± standard deviation (n = 3). *
 298 Values of viscosity at 1000 s⁻¹ were calculated by extrapolation of the data.

299 The correlation between apparent viscosity and shear rate of the polysaccharide solutions is
 300 reported in **Fig. 2B**. A shear-thinning behavior was observed for all polysaccharide solutions,
 301 indicating that the apparent viscosity decreased as the shear rate increased. According to Hos-
 302 seini, Ghaderi & Gómez-Guillén, (2020); Pamies, Schmidt, Martínez & Garcia De la Torre,
 303 (2010) and Sharmin, Sone, Walsh, Sivertsvik & Fernández, (2021), the decrease in viscosity

304 as shear rate increases can be explained by the theory of disentanglement. The breakdown of
305 the polysaccharide molecular structure due to shear stress leads to a reduction of the interac-
306 tions between adjacent chains. At a shear rate of 10 s^{-1} , MC, CHI and HPMC presented the
307 higher apparent viscosity ($\geq 2 \text{ Pa}\cdot\text{s}$) among all the polysaccharides evaluated, while the other
308 polysaccharide solutions exhibited at the same shear rate an apparent viscosity lower than 0.3
309 $\text{Pa}\cdot\text{s}$. The values of apparent viscosity were also extrapolated to predict the apparent viscosity
310 of the solutions at a shear rate of 1000 s^{-1} . This allows comparison to be made when high
311 shear rates are applied to coatings during different unit operations at industrial scale. Based
312 on these extrapolated data, it can be estimated that, at a shear rate of 1000 s^{-1} , polysaccharide
313 solutions will present in all cases an apparent viscosity lower than $0.5 \text{ Pa}\cdot\text{s}$.

314 In the preparation of self-standing films using polysaccharide solutions by the solvent casting
315 method, viscosity was not a critical parameter to consider since at relatively low polymer
316 concentrations, the solutions efficiently spread over the surface area of a petri dish to produce
317 films at the lab scale (data not shown). However, polysaccharide film-forming solutions can
318 also be used to coat different materials, such as paper or plastics. For coating, the rheological
319 behavior of the solution is an important parameter to be considered, especially for further
320 industrial applications since it determines the design of the different unit operations and pro-
321 cesses involved in the coating process as well as the performance of the coating. The targeted
322 apparent viscosity of a biopolymer solution for coating applications at industrial scale de-
323 pends on different factors and, particularly, the method used for the coating operation. Meth-
324 ods such as dip-coating require high viscosity values ($> 10 \text{ Pa}\cdot\text{s}$) since low shear rate values
325 are applied ($< 10 \text{ s}^{-1}$), whereas techniques such as brushing or rolling may require lower vis-
326 cosity values ($< 0.5 \text{ Pa}\cdot\text{s}$) since high shear rate values are applied to the solutions ($> 1000 \text{ s}^{-1}$)
327 (Fluidan, 2018). Therefore, the polysaccharide solutions, with the concentration used in this
328 study could not be suitable for applications like dip-coating since their viscosity at low shear
329 rates was lower than $3 \text{ Pa}\cdot\text{s}$. However, they could preferably be used for applications such as
330 brushing and rolling as their viscosity was estimated to be less than $0.5 \text{ Pa}\cdot\text{s}$ at a shear rate of
331 1000 s^{-1} .

332 **A.**



333 **B.**

334 **Fig. 2.** Rheological properties of polysaccharide solutions at a concentration of 2 % (w/w). **A.** Shear stress (τ) as a function
 335 of shear rate ($\dot{\gamma}$) of polysaccharide solutions measured at $25(\pm 1)$ °C. Dotted lines represent the fitted curves based on the
 336 Ostwald de Waele model. n_{ost} indicates the n value given by the model for each curve. **B.** Apparent viscosity (μ_{app}) as a func-
 337 tion of shear rate of polysaccharide solutions, measured at $25(\pm 1)$ °C. Values of the apparent viscosity at 1000 s^{-1} were
 338 calculated by extrapolation of the data. **HPMC:** Hydroxypropyl Methylcellulose. **MC:** Methyl Cellulose. **HPC:** Hydroxy-
 339 propyl Cellulose. **LMP:** Low Methoxyl Pectin. **CS:** Cationic Starch. **SA:** Sodium Alginate. **KC:** Kappa-Carrageenan (*:
 340 Temperature of measurement $70(\pm 1)$ °C). **CHI:** Chitosan. **PL:** Pullulan. Values are reported as mean \pm standard deviation (n
 341 = 3).

342 **3.1.2. Surface properties of film-forming solutions**

343 The surface tension of the polysaccharide solutions, including their polar and dispersive
 344 components, were measured at 25 °C. Results are displayed in **Table 3**. Among all polysac-
 345 charides analyzed, CS showed the highest surface tension (63 mN.m⁻¹), while HPC showed
 346 the lowest one (39 mN.m⁻¹). It is also noteworthy that the cellulose derivatives HPMC, MC
 347 and HPC ranged among the lowest values (lower than 45 mN.m⁻¹). For the other polysaccha-
 348 ride solutions, the surface tension was always higher than 50 mN.m⁻¹. In all polysaccharide
 349 solutions, the polar component represented more than 48 % of the total surface tension. This
 350 high level of polar interactions was expected due to the hydrophilic nature of polysaccha-
 351 rides.

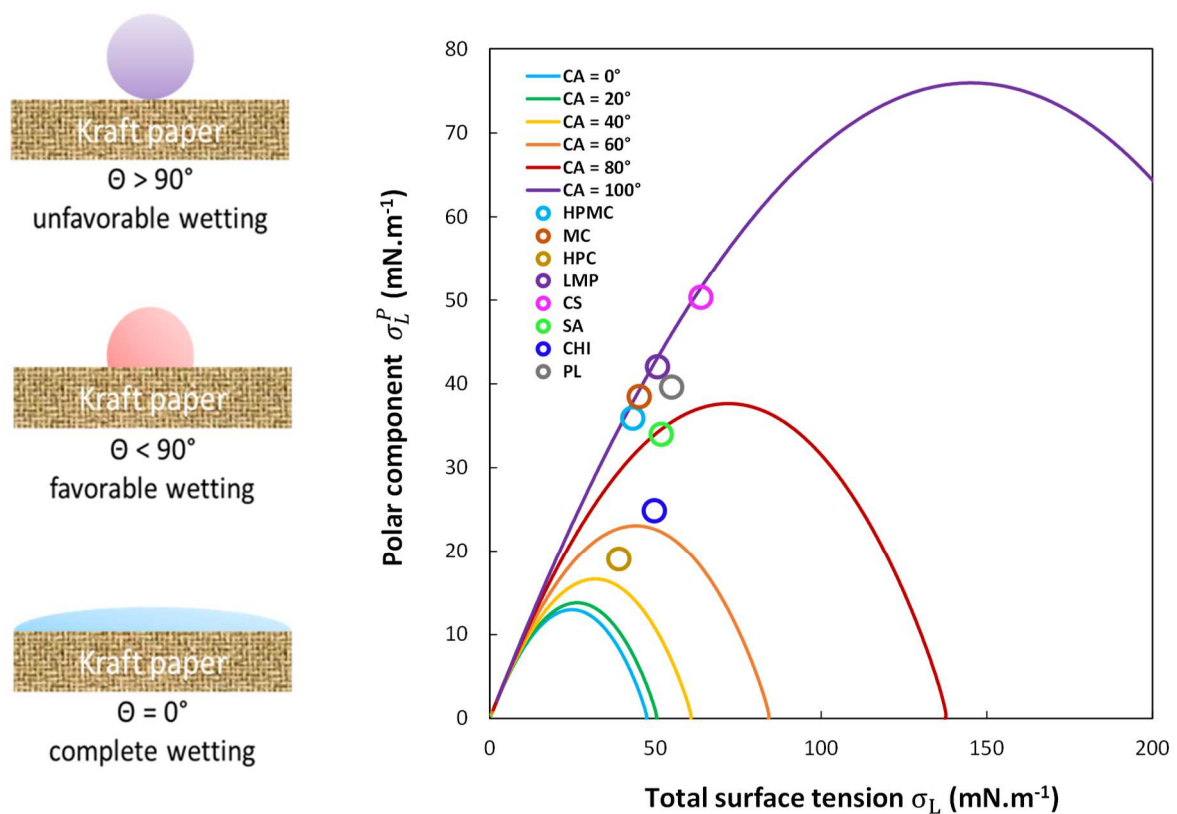
352 **Table 3.** Surface tension, with polar and dispersive components, of polysaccharide solutions at 25 °C.

Polysaccharide	Total surface tension	Dispersive component	Polar component	Polar %
	σ_L (mN.m ⁻¹)	σ_L^d (mN.m ⁻¹)	σ_L^p (mN.m ⁻¹)	
HPMC	43.2±0.5	7.3±0.7	35.9±0.7	83.1
MC	45.1±0.5	6.6±0.8	38.5±0.8	85.2
HPC	38.9±0.8	19.9±0.8	19.0±0.8	48.8
LMP	50.6±1.1	8.6±0.6	42.0±0.6	83.1
CS	63.7±2.4	13.4±1.5	50.3±1.5	70.9
SA	51.8±0.2	17.8±1.4	34.0±1.4	65.6
*KC	N/A	N/A	N/A	N/A
CHI	49.7±0.6	24.8±0.8	24.9±0.8	50.0
PL	54.9±0.2	15.3±2.4	39.6±2.4	72.1

353 **HPMC:** Hydroxypropyl Methylcellulose. **MC:** Methyl Cellulose. **HPC:** Hydroxypropyl Cellulose. **LMP:** Low Methoxyl
 354 Pectin. **CS:** Cationic Starch. **SA:** Sodium Alginate. ***KC:** Kappa-Carrageenan (N/A: not applicable due to gelation at 25 °C).
 355 **CHI:** Chitosan. **PL:** Pullulan. Values are reported as mean ± standard deviation (n = 3).

356 The interactions between a liquid and a solid are of great importance since they determine the
 357 wetting properties of the liquid on the surface. As an example, industrial processes like coat-
 358 ing and printing of paper and board are complex procedures involving spreading and absorb-
 359 ing a liquid into the fiber network. Predicting the wettability and adhesion of a liquid on a
 360 specific surface requires information about the polar and dispersive interactions of both the
 361 liquid and the solid. Indeed, they will determine the contact angle formed between the two
 362 components. As shown in **Fig. 3A**, liquids giving a contact angle equal to 0° are classified as
 363 having "complete wettability" of the solid surface, while those whose contact angle lie be-
 364 tween 0° and 90° are classified as having "favorable wetting". Those which present a contact
 365 angle above 90° are classified as having "unfavorable wetting" (Fathi Azarbayjani, Jouyban
 366 & Chan, 2009).

367 The determination of the so-called "wetting envelope" provides the wettability for current or
 368 future coatings, as any liquids whose polar and dispersed components lie within the contour
 369 for a particular contact angle will wet the corresponding solid surface with the contact angle
 370 of this contour (Chen, Cheng & Lee, 2021). For this study, the wetting envelope of a Kraft
 371 paper, reported by Saraiva et al. (2010) as having a total surface tension of $47.4 \text{ mN}\cdot\text{m}^{-1}$, with
 372 a polar component of $0.1 \text{ mN}\cdot\text{m}^{-1}$ and a dispersive component of $47.3 \text{ mN}\cdot\text{m}^{-1}$, was plotted to
 373 compare the wettability of the different polysaccharide solutions on that specific surface.
 374 Kraft paper was selected as a support due to its common applications for the packaging of
 375 flour, sugar, dried fruits and vegetables (Deshwal et al., 2019). The wetting envelope of Kraft
 376 paper and the wettability of polysaccharide solutions on this surface are displayed in **Fig. 3B**.



377 **A.** **B.**
 378 **Fig. 3.** A. Schematic diagram of contact angle and wettability behavior. B. Wetting envelope with 0°, 20°, 40°, 60°, 80° and
 379 100° contours of an uncoated paper (80 g/m²) produced with a Eucalyptus globulus Kraft pulp and wettability of the poly-
 380 saccharide solutions on the surface of Kraft paper at 25 °C. Values of the surface tension of Kraft paper were taken from
 381 Saraiva et al. (2010). θ : contact angle. **HPMC**: Hydroxypropyl Methylcellulose. **MC**: Methyl Cellulose. **HPC**: Hydroxy-
 382 propyl Cellulose. **LMP**: Low Methoxyl Pectin. **CS**: Cationic Starch. **SA**: Sodium Alginate. **CHI**: Chitosan. **PL**: Pullulan.

383 According to this wetting envelope, HPC is the polysaccharide solution that would have the
 384 lowest contact angle ($< 60^\circ$) once deposited onto Kraft paper, followed by CHI and SA ($<$

385 80°), then by HPMC, MC, LMP, PL and CS with a contact angle higher than 90°. This means
386 that polysaccharide solutions such as HPC, CHI, and SA would spread well and wet the sur-
387 face of Kraft paper since they are in the range of liquids with favorable wetting ($\theta < 90^\circ$). In
388 contrast, solutions such as HPMC, MC, LMP, PL and CS would only establish a few interac-
389 tions with the surface of Kraft paper. They would have an unfavorable wetting ($\theta > 90^\circ$) that
390 may lead to heterogeneous thickness, holes or crack formation.

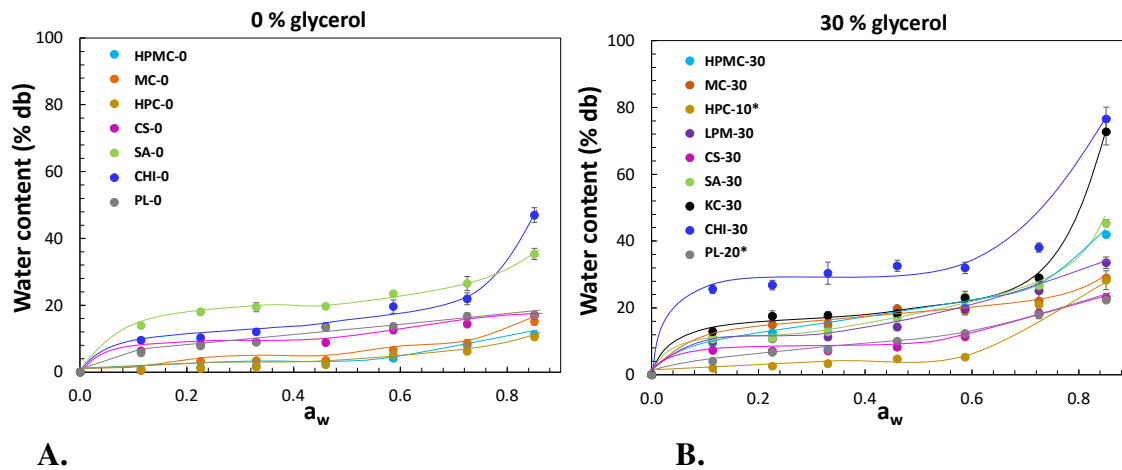
391 Liquids with similar total surface tension σ_L can thus have a different contact angle with the
392 solid, as observed for the different polysaccharide solutions studied. HPC and HPMC solu-
393 tions displayed a similar total surface tension, 38.9 and 43.2 mN.m⁻¹, respectively. However,
394 the wetting envelope of Kraft paper showed that HPC would form a contact angle just below
395 60°, whereas HPMC would give a contact angle of more than 90°. This can be explained by
396 the fact that the ratio between the dispersive and polar components of the HPC solution is
397 different from that of the HPMC solution. Polar components accounted for 49 % of the sur-
398 face tension of HPC, while they represented 83 % for HPMC. Therefore, Kraft paper would
399 form more interactions with a low-polar solution since its structure is mostly dispersive.

400 **3.2. Functional properties of polysaccharide films as self-standing materials**

401 **3.2.1. Water sorption isotherm of films**

402 Water sorption isotherms of polysaccharide films without glycerol and with 30 % of glycerol
403 at 25 ° C are displayed in **Fig. 4**. First, polysaccharides films without addition of glycerol
404 (**Fig. 4A**) started to significantly sorb water at a relative humidity of 60 %. CHI and SA
405 demonstrated the highest sensitivity to moisture, even at low relative humidity. The moisture
406 sorption of these films increased by a factor two from 60 % to 85 % relative humidity. The
407 water content of these two polysaccharides increased from 19.6 and 23.4 % to 46.9 and 35.3
408 %, respectively. This is in agreement with the values previously reported by Monte, Moreno,
409 Senna, Arrieche & Pinto, (2018) for CHI and Xiao & Tong, (2013) for SA films. These au-
410 thors also evidenced a slow increase in the moisture content of CHI and SA films up to a rela-
411 tive humidity of 60 %. Above this threshold value, a slight increase in the relative humidity
412 led to a significant increase in the moisture content of the films. Such phenomenon occurs
413 because the first water molecules that enter the polymer loosen the structure and make it easi-
414 er for subsequent molecules to enter the polymer network (Su et al., 2010). The presence of
415 functional groups such as hydroxyl (-OH), glycosidic linkage (C-O-C) as well as amino
416 (NH₂, in the form of NH₃⁺) in the case of CHI films (Crouvisier-Urien et al., 2016; Made-
417 leine-Perdrillat et al., 2016) and carboxylic groups (-COOH) in SA films, confers to these

418 polysaccharides. a high affinity for water molecules. In contrast, the cellulose derivatives
 419 (HPMC, MC and HPC) showed to be the polysaccharides with the lowest sensitivity to mois-
 420 ture sorption. At a relative humidity of 11 %, they presented a moisture content 7 to 17 times
 421 lower than the other polysaccharides. They also showed to be less affected by an increase in
 422 the relative humidity. This lower affinity to water presented by the cellulose derivatives may
 423 be due to the presence of methyl groups (-CH₃) that have replaced part of the hydroxyls (-
 424 OH) (Nasatto et al., 2015), thus decreasing their hydrophilicity.



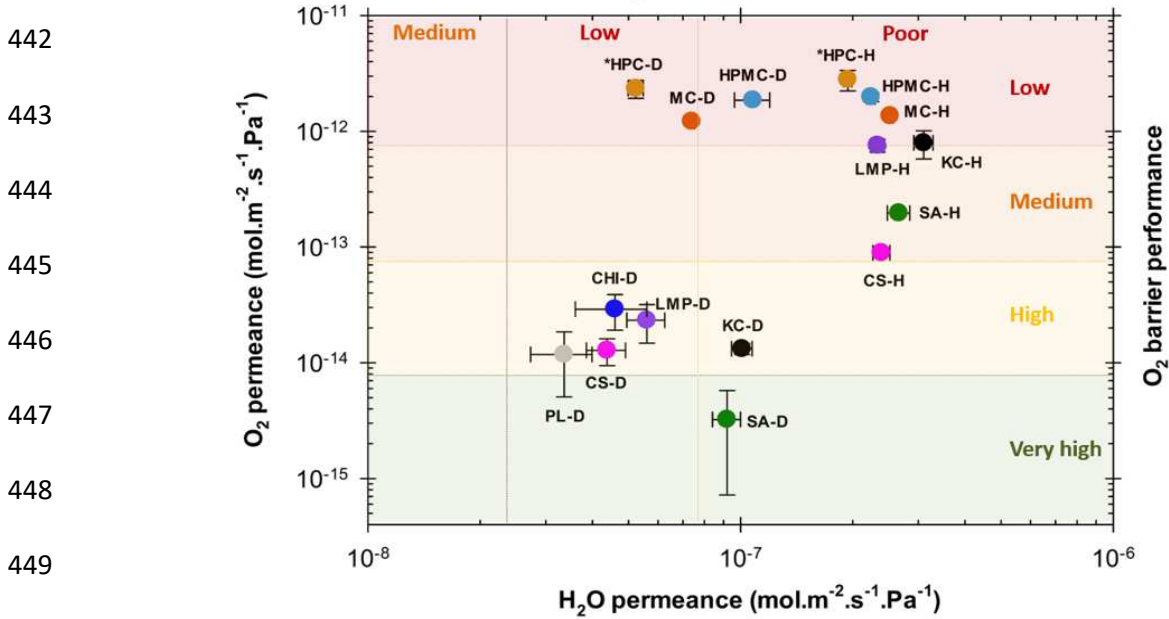
425 **A.** **B.**
 426 **Fig. 4.** Moisture sorption isotherms of polysaccharide films displaying the water content of the films (expressed as percent-
 427 age of the dry basis) according to the water activity (a_w). **A.** Films without glycerol. LMP-0 and KC-0 were not measured
 428 due to brittleness of the films. **B.** Films containing 30 % glycerol (*except HPC with 10 % and PL with 20 %). Dotted lines
 429 are a guide for the eyes. **HPMC:** Hydroxypropyl Methylcellulose. **MC:** Methyl Cellulose. **HPC:** Hydroxypropyl Cellulose.
 430 **LMP:** Low Methoxyl Pectin. **CS:** Cationic Starch. **SA:** Sodium Alginate. **KC:** Kappa-Carrageenan. **CHI:** Chitosan. **PL:**
 431 Pullulan. Values are reported as mean \pm standard deviation (n = 3).

432 The addition of 30 % of glycerol to the films (**Fig. 4B**) increased the moisture content by a
 433 factor of two for polysaccharides such as CHI, MC and HPMC. Such phenomenon has al-
 434 ready been highly reported in the literature (Choi, Kim, Hanna, Weller & Kerr, 2008; Su et
 435 al., 2010). This occurs because glycerol not only loosens the microstructure of the films, but
 436 also increases their hydrophilicity (Choi et al., 2008). For the other polysaccharides, such as
 437 HPC, SA, CS and PL, the effect was less pronounced.

438 3.2.2. Barrier properties of films

439 The oxygen permeance as a function of the water vapor permeance of the polysaccharide
 440 films under two different relative humidity differentials is displayed in **Fig. 5**.

441 A.



449 B.

Barrier performance	Oxygen permeance	Water vapor permeance
	mol.m ⁻² .s ⁻¹ .Pa ⁻¹	mol.m ⁻² .s ⁻¹ .Pa ⁻¹
Very high	< 7.6x10 ⁻¹⁵	< 7.6x10 ⁻¹²
High	7.6x10 ⁻¹⁵ - 7.6x10 ⁻¹⁴	1.0x10 ⁻⁰⁹ - 1.0x10 ⁻⁰⁸
Medium	7.6x10 ⁻¹⁴ - 7.6x10 ⁻¹³	1.0x10 ⁻⁰⁸ - 2.6x10 ⁻⁰⁸
Low	7.6x10 ⁻¹³ - 7.6x10 ⁻¹²	2.6x10 ⁻⁰⁸ - 7.8x10 ⁻⁰⁸
Poor	> 7.6x10 ⁻¹²	> 7.8x10 ⁻⁰⁸

451 **Fig. 5.** Barrier properties of polysaccharide films to water vapor and oxygen. **A.** Oxygen permeance (P_{O_2}) as a function of
 452 the water vapor permeance (P_{H_2O}) of polysaccharide films with 20 % of glycerol (*Except HPC films with 10 % of glycerol)
 453 under two different relative humidity conditions at 25 °C. Semi-dry condition (indicated with a D) corresponds to: P_{H_2O} (0
 454 %-50 % RH differential), P_{O_2} (50 % RH). Humid condition (indicated with an H) corresponds to: P_{H_2O} (50 %-100 % RH),
 455 P_{O_2} (80 % RH). **HPMC:** Hydroxypropyl Methylcellulose. **MC:** Methyl Cellulose. **HPC:** Hydroxypropyl Cellulose. **LMP:**
 456 Low Methoxyl Pectin. **CS:** Cationic Starch. **SA:** Sodium Alginate. **CHI:** Chitosan. **PL:** Pullulan. Values are reported as
 457 mean \pm standard deviation. (n = 3 for P_{O_2} , n = 4 for P_{H_2O}). Detailed values are provided in **Appendix A.** **B.** Classification of
 458 the O_2 and H_2O barrier performance of polysaccharide films. The classification of the O_2 and H_2O barrier performance,
 459 referred to as poor, low, medium, high and very high, was adapted from Wu et al. (2021). For practical purpose, the oxygen
 460 permeance value (mol.m⁻².s⁻¹.Pa⁻¹) can be simply converted into OTR (cm³.m⁻².day⁻¹) by multiplying the value by
 461 2.09x10¹⁴. For conversion of the water vapor permeance (mol.m⁻².s⁻¹.Pa⁻¹) into WVTR (g.m⁻².day⁻¹) the value can be multi-
 462 plied by 2.46x10⁹. The partial pressure differential used for the permeance measurement was 1000 hPa for oxygen and 1584
 463 Pa for water vapor.

464 Regarding the permeance to oxygen, the cellulose derivatives HPMC, MC and HPC appeared
 465 to be the most permeable polysaccharides under both humid and semi-dry conditions (>
 466 1.1×10^{-12} mol.m⁻².s⁻¹.Pa⁻¹). A decrease of less than 17 % was observed in the permeance to

467 oxygen for the three cellulose derivatives from humid to semi-dry condition. They also
468 showed to be the least affected by changes in the relative humidity conditions, as previously
469 evidenced by the moisture sorption isotherms presented in **Fig. 4**. This higher oxygen perme-
470 ance of the films from the three cellulose derivatives (HPMC, MC and HPC) compared with
471 other polysaccharide films could be a consequence of the presence of bulky side groups that
472 generate a larger fractional free volume (Lagaron, Catalá & Gavara, 2004). In addition, the
473 presence of methyl groups (-CH₃), which are non-polar functional groups, could also contrib-
474 ute to a greater affinity of the films with oxygen molecules, which are also non-polar, thus
475 facilitating their transfer through the films. Furthermore, in the case of HPC, the hydroxypro-
476 pyl pendant groups may generate more steric hindrance than the methyl groups of MC and, to
477 a lesser extent, HPMC, leading to a less compact polymer network and higher oxygen perme-
478 ance.

479 For all the other polysaccharides, a significant decrease in the oxygen permeance (> 85 %)
480 was observed when going from humid to semi-dry condition. In particular, the oxygen per-
481 meance of SA, KC and LMP, decreased by more than 97 %. Under humid condition, CS pre-
482 sented the lowest permeance to oxygen (8.9×10^{-14} mol.m⁻².s⁻¹.Pa⁻¹), followed by SA
483 (2.0×10^{-13} mol.m⁻².s⁻¹.Pa⁻¹), LMP (7.6×10^{-13} mol.m⁻².s⁻¹.Pa⁻¹), and KC (8.0×10^{-13}
484 mol.m⁻².s⁻¹.Pa⁻¹), respectively. The order changed under semi-dry condition, with SA pre-
485 senting the lowest permeance to oxygen (3.2×10^{-15} mol.m⁻².s⁻¹.Pa⁻¹), followed by PL
486 (1.2×10^{-14} mol.m⁻².s⁻¹.Pa⁻¹), CS and KC (1.3×10^{-14} mol.m⁻².s⁻¹.Pa⁻¹ for both of them), LMP
487 (2.3×10^{-14} mol.m⁻².s⁻¹.Pa⁻¹) and CHI (2.9×10^{-14} mol.m⁻².s⁻¹.Pa⁻¹), respectively. Concerning
488 the water vapor permeance, a significant decrease (> 50 %) was observed for all polysaccha-
489 rides from humid to semi-dry condition. In humid condition, the values ranged from 1.9 to
490 3.1×10^{-7} mol.m⁻².s⁻¹.Pa⁻¹, while in semi-dry condition, their permeance values were widely
491 spread, with PL having the lowest water vapor permeance (3.4×10^{-8} mol.m⁻².s⁻¹.Pa⁻¹) and
492 KC having the highest one (1.8×10^{-7} mol.m⁻².s⁻¹.Pa⁻¹).

493 As expected, the permeance to oxygen and water vapor of the polysaccharides was always
494 significantly higher when the films were exposed to high relative humidity. This is because
495 water induces a plasticizing or swelling effect on polymers that increases the molecular free
496 volume and, therefore the gas permeability (Wang et al., 2018). However, this plasticizing
497 effect brought by water molecules is not the same for all polymers since they do not sorb wa-
498 ter at the same level, as evidenced by the moisture sorption isotherms displayed in **Fig. 4**. The
499 variations in oxygen and water vapor permeance between the different polysaccharide films

500 result from different cohesive energy densities, free volume, and degree of crystallinity in the
501 matrix (Khalil et al., 2019). Materials with good resistance to oxygen often have high number
502 of polar interactions and hydrogen bonding, which usually results in high hydrophilicity and,
503 thus, poor water vapor barrier (Wang et al., 2018).

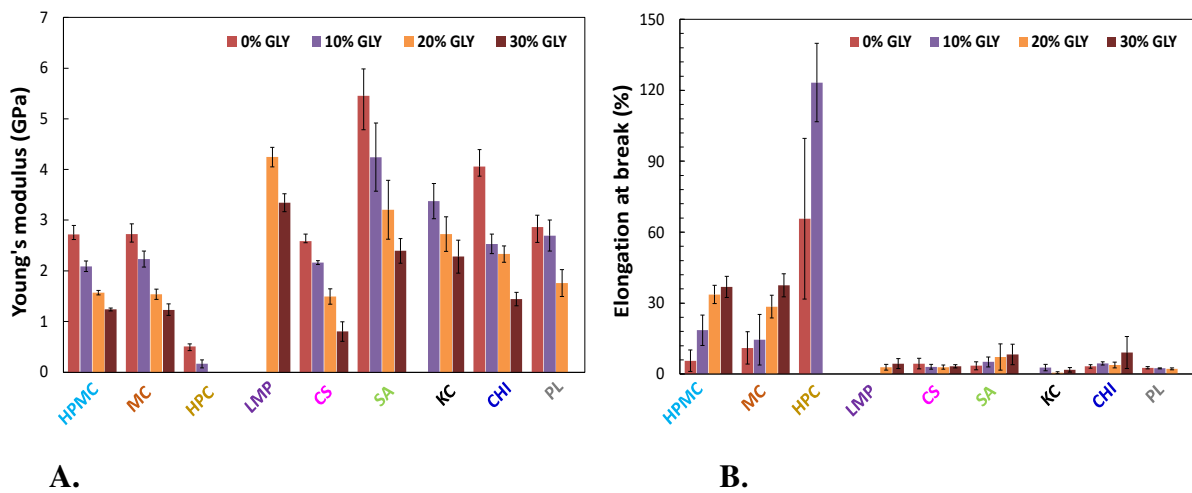
504 In order to evaluate the performance of the polysaccharide films, the classification proposed
505 by Wu, Misra & Mohanty, (2021) for biodegradable polymers according to their barrier prop-
506 erties was used and it is displayed in **Fig. 5A**. Detailed values of this classification are pre-
507 sented in **Fig. 5B**. According to this classification, SA in semi-dry condition showed a "very
508 high" barrier against oxygen ($P_{O_2} < 7.6 \times 10^{-15} \text{ mol.m}^{-2}.\text{s}^{-1}.\text{Pa}^{-1}$). This lie within the same range
509 as certain conventional plastics with very good oxygen barrier such as EVOH ($\sim 2.3 \times 10^{-15}$
510 $\text{mol.m}^{-2}.\text{s}^{-1}.\text{Pa}^{-1}$) and PVDC ($\sim 4.7 \times 10^{-15} \text{ mol.m}^{-2}.\text{s}^{-1}.\text{Pa}^{-1}$) and to that of biodegradable plas-
511 tics like polyglycolic acid (PGA) ($\sim 4.7 \times 10^{-15} \text{ mol.m}^{-2}.\text{s}^{-1}.\text{Pa}^{-1}$), which has been considered
512 as one of the highest barrier polymers that can be biodegraded (Wu et al., 2021). However, as
513 previously noted, the relative humidity plays an important role in the oxygen and water vapor
514 barrier properties of the polysaccharide films. SA shifted from a "very high" barrier against
515 oxygen in semi-dry condition to a "medium" barrier (P_{O_2} between 7.6×10^{-14} and 7.6×10^{-13}
516 $\text{mol.m}^{-2}.\text{s}^{-1}.\text{Pa}^{-1}$) in humid condition. The other polysaccharides also moved from "high" (P_{O_2}
517 between 7.6×10^{-15} and $7.6 \times 10^{-14} \text{ mol.m}^{-2}.\text{s}^{-1}.\text{Pa}^{-1}$) barrier in semi-dry condition to a "medi-
518 um" barrier in humid condition, except for the cellulose derivatives (HPMC, MC and HPC),
519 which showed a "low" (P_{O_2} between 7.6×10^{-13} and $7.6 \times 10^{-12} \text{ mol.m}^{-2}.\text{s}^{-1}.\text{Pa}^{-1}$) barrier against
520 oxygen at both humid and semi-dry conditions and KC which moved from "high" to "low"
521 barrier. Regarding the barrier property against water vapor, all polysaccharides showed a
522 "poor" barrier ($P_{H_2O} > 7.8 \times 10^{-8} \text{ mol.m}^{-2}.\text{s}^{-1}.\text{Pa}^{-1}$) in humid condition and a "low" barrier
523 (P_{H_2O} between 2.6×10^{-8} and $7.8 \times 10^{-8} \text{ mol.m}^{-2}.\text{s}^{-1}.\text{Pa}^{-1}$) in semi-dry condition, except for
524 HPMC, SA and KC which also exhibited a "poor" barrier in semi-dry condition.

525 Although the plasticizing effect of glycerol is not discussed in detail in this part of the work,
526 the oxygen and water vapor permeance of the polysaccharide films containing different glyc-
527 erol concentrations are provided in **Appendix A**.

528 **3.2.3. Mechanical properties of films**

529 Young's modulus and the elongation at break of the polysaccharide films with different per-
530 centages of glycerol were measured and are displayed in **Fig. 6**.

531 Regarding the Young's modulus of the films (**Fig. 6A**) without addition of glycerol, values
 532 ranged from 0.5 to 5.5 GPa. HPC was the polysaccharide that presented the lowest Young's
 533 modulus of all polysaccharides (0.5 GPa). It was followed by CS (2.6 GPa), HPMC (2.7
 534 GPa), MC (2.7 GPa), PL (2.9 GPa), CHI (4.1 GPa) and finally SA, which exhibited the high-
 535 est Young's modulus value (> 5 GPa). Polysaccharides such as LMP and KC could not be
 536 measured when no plasticizer was added due to their brittleness. When glycerol was added to
 537 the films, Young's modulus decreased in all cases due to the plasticization effect. This de-
 538 crease was greater than 54 % for HPMC, MC, CHI, CS and SA when the glycerol concentra-
 539 tion increased from 0 % to 30 %.



540 **A.** **B.**
 541 **Fig. 6.** Mechanical properties of polysaccharide films at 25 °C and 50 % RH with different glycerol percentages (0, 10, 20
 542 and 30 %). **(A).** Young's modulus (GPa). **(B).** Elongation at break (%). **HPMC:** Hydroxypropyl Methylcellulose. **MC:** Me-
 543 thyl Cellulose. **HPC:** Hydroxypropyl Cellulose. **LMP:** Low Methoxyl Pectin. **CS:** Cationic Starch. **SA:** Sodium Alginate.
 544 **KC:** Kappa-Carrageenan. **CHI:** Chitosan **PL:** Pullulan. Values are reported as mean \pm standard deviation (n = 6). Detailed
 545 values are provided in **Appendix B.**

546 The elongation at break of the films is presented in **Fig. 6B**. Without glycerol, HPC films
 547 showed the highest elongation at break (65 %), with the longest plastic deformation com-
 548 pared with the other polysaccharides. It was followed by the other cellulose derivatives MC
 549 and HPMC, with more than 5 % of elongation. The other polysaccharides displayed an elon-
 550 gation of less than 5 %, thus being less stretchable and more brittle than the cellulose deriva-
 551 tives. When glycerol was added to the films, a strong increase in the elongation at break was
 552 observed for most of the films. The cellulose derivatives HPMC, MC and HPC presented an
 553 increase of 555 %, 239 % and 87 %, respectively, when glycerol was added (from 0 % to 30
 554 % for HPMC and MC and from 0 % to 10 % for HPC). Both SA and CHI showed an in-

555 crease, higher than 138 % when glycerol was added from 0 % to 30 %. For the other polysac-
556 charides, LMP, CS, KC and PL, the plasticizing effect was found not to be significant. In the
557 case of HPC and PL, the addition of glycerol was even limited to 10 % and 20 % (w/w), re-
558 spectively, as above this concentration, phase separation occurred in the films.

559 The use of a plasticizer is required in most of the cases, to improve the mechanical properties
560 of biopolymer films. Their brittleness and stiffness are due to extensive interactions between
561 polymer chains such as intermolecular bonds that lead to high mechanical cohesion between
562 chains (Jantrawut, Chaiwarit, Jantanasakulwong, Brachais & Chambin, 2017; Jarray, Gerbaud
563 & Hemati, 2016). The higher this mechanical cohesion, the stiffer the polymer network. Plas-
564 ticizers, such as glycerol, decrease the cohesion within the polymer network by reducing
565 these intermolecular forces between adjacent polymer chains and substituting them with hy-
566 drogen bonds formed between the plasticizer and the polymer chains (Immergut & Mark,
567 1965). However, plasticizers do not follow the same behavior in all biopolymer matrices. The
568 efficiency of a plasticizer depends on the polymer properties, such as the molecular weight,
569 the chemical composition (Avella et al., 2007), the rate of plasticizer diffusion into the poly-
570 mer matrix (Sothornvit & Krochta, 2005), and the type of interaction (intramolecu-
571 lar/intermolecular) between the polymer and the plasticizer (Smith, Escobar, Andris, Board-
572 man & Peters, 2021). These parameters generally vary between polymers, leading to a com-
573 pletely different compatibility and, therefore, a different plasticizing effect. It is also worth
574 noting that even though the use of glycerol as plasticizer improves the mechanical properties
575 of the polysaccharide films, these changes remain in a rather limited range and are not even
576 significant enough in some cases to drastically improve the performance of the films. There-
577 fore, it can be concluded that the mechanical behavior of the films is predominantly governed
578 by the polymer molecular structure, rather than by the effect of the plasticizer. Furthermore,
579 although the different mechanical behaviors observed for polysaccharide films are related to
580 structural factors (such as degree of substitution, crystallinity, free volume, thermal history,
581 molecular orientation, etc.), it is very difficult to establish a link with a single parameter.
582 Even considering only cellulose derivatives, as also reported by Espinoza-Herrera, Pedroza-
583 Islas, San Martín-Martínez, Cruz-Orea & Tomás, (2011), the differences between polysaccha-
584 rides cannot be explained merely by the degree of substitution or the percentage of crystal-
585 linity, but would require extensive multiparametric analysis.

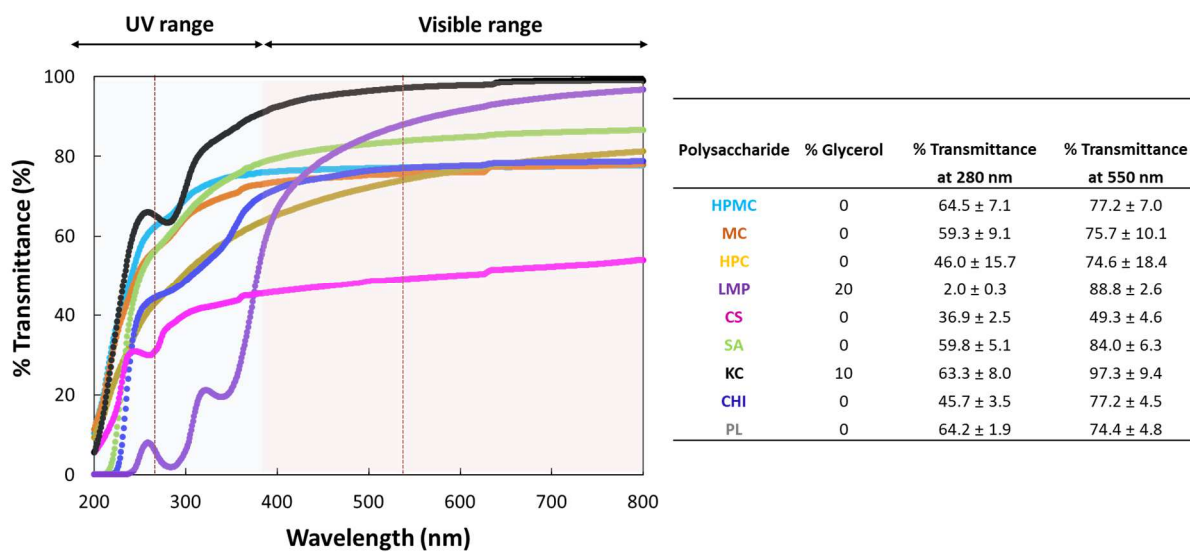
586 Moreover, it should be noticed that, for coating applications, the mechanical properties of
587 polysaccharides are less critical because the mechanical support is mostly provided by the

588 material on which the polysaccharide is coated (for example, paper). However, the mechani-
 589 cal properties remain important parameters for the selection of the polysaccharide coating
 590 since the material must preserve its structure during any further manipulation in order to en-
 591 sure the efficiency of the coating and the preservation of the properties over time.

592 3.2.4. Transparency and UV-blocking ability of films

593 The transparency and UV blocking ability of the polysaccharide films were measured by the
 594 percentage of transmittance in the 200-800 nm wavelength range. Although the UV light
 595 ranges between 200-380 nm, for convenience purpose, the transmittance at 280 nm was se-
 596 lected to compare the UV blocking ability of the films. Similarly, at a wavelength of 550 nm,
 597 the transmittance was chosen for comparing the quantity of visible light that can pass through
 598 the films (transparency). Transmittance values at the different wavelengths obtained for the
 599 polysaccharide films are displayed in Fig. 7.

600 All the polysaccharide films showed good transparency since the transmittance at 550 nm
 601 was higher than 74 %, except for CS, whose transmittance was less than 50 %. Of all poly-
 602 saccharides, KC showed the highest transparency (97 %), followed by LPM (89 %), SA (84
 603 %), CHI (77 %), HPMC, MC, HPC, and PL (from 77 to 75 % respectively) and, lastly, CS
 604 with 50 %. Regarding the UV screening capacity, polysaccharide films showed a transmit-
 605 tance lower than 65 % in all cases. LMP was the polysaccharide with the lowest transmit-
 606 tance (2 %). It was followed by CS (37 %), CHI and HPC (46 % for both), MC and SA (59 %



607 for both) and lastly KC, PL and HPMC (from 63 to 65 % respectively).

608 **Fig. 7.** UV-Visible transmission spectra of polysaccharide films and values of transmittance at 280 nm (UV range) and 550
609 nm (Visible range) at 25 °C. **HPMC:** Hydroxypropyl Methylcellulose. **MC:** Methyl Cellulose. **HPC:** Hydroxypropyl Cellu-
610 lose. **LMP:** Low Methoxyl Pectin. **CS:** Cationic Starch. **SA:** Sodium Alginate. **KC:** Kappa-Carrageenan. **CHI:** Chitosan.
611 **PL:** Pullulan. Values are reported as mean \pm standard deviation (n = 3).

612 Of particular interest is pectin which has also previously been reported by Shankar, Tanom-
613 rod, Rawdkuen & Rhim, (2016) and Younis, Abdellatif, Ye & Zhao, (2020) as a good UV
614 barrier polysaccharide, avoiding more than 70 % of incident UV light. The origin of this UV
615 protection arising in pectin is not well known in the literature. However, such behavior of
616 pectin against UV light might be related to their functional role in the cell wall of fruits and
617 vegetables, these products being constantly exposed to ultraviolet radiation and requiring
618 protection to avoid photo-oxidation.

619 The level of transparency of packaging materials influences the perception and acceptability
620 of consumers. The level required for a material depends mostly on its application. On the
621 contrary, the UV screening capacity of food packaging materials is a critical parameter since
622 UV radiation (200-400 nm) can promote lipid photo-oxidation mechanisms in many food
623 products. It can also damage photosensitive substances such as pigments and vitamins (Sun
624 Lee, L.Yam & PierGiovanni, 2008). Moreover, UV radiation can cause photooxidative degra-
625 dation leading to a break in the polymer chain that reduces molecular weight, causing deterio-
626 ration of mechanical properties, and resulting in inefficient materials after an unpredictable
627 period (Yousif & Haddad, 2013).

628 **3.2.5. Correlations between functional properties**

629 The functional properties of polymers depend on many factors related to the polymer struc-
630 ture, including cohesive energy density, free volume, degree of crystallinity, orientation and
631 degree of cross-linking (Abdan et al., 2020). Although some obvious correlations can be ob-
632 served when considering the change in functional properties as a function of plasticizer con-
633 centration for a given polymer, there is no direct correlation when it comes to the different
634 polysaccharides studied in this work. Taking into account all polysaccharides together at the
635 same glycerol concentration and the same water activity, there are no further correlations be-
636 tween the measured properties. For example, the barrier properties (to oxygen and water va-
637 por) correlate neither with the mechanical properties (Young's modulus, elongation at break
638 and tensile strength) nor with the polar/dispersive ratio of the surface tension, as expected.
639 Even when considering the cohesive energy density and the solubility parameter of the poly-
640 mers, calculated by the group contribution method (Table 1), these are not explanatory pa-

641 rameters of the measured macroscopic properties as no clear correlation can be found. There-
642 fore, when dealing with polysaccharides having different chemical structures and thus various
643 film-forming mechanisms, the relationships between molecular-scale parameters and macro-
644 scopic functional properties are likely multiparametric and remain a critical issue to be fur-
645 ther addressed. Although some studies have already identified tentative correlations for the
646 same polymer as a function of the degree of substitution (Elidrissi, 2012) or the degree of
647 crystallinity (Udayakumar et al., 2020), for the time being there is no ubiquitous model that
648 can be applied to all polymers.

649 **4. Conclusions**

650 This study provides an extensive experimental review of the main functional properties of the
651 most promising polysaccharides for potential application in the field of food packaging. Their
652 permeability to water vapor and to oxygen, as well as their mechanical and optical properties
653 were measured under standardized conditions for polysaccharide films with different percent-
654 ages of glycerol used as a plasticizer. Film-forming solutions were also characterized for their
655 viscosity and surface tension properties. Regarding water vapor barrier property, all polysac-
656 charide films showed rather low performance, due to their hydrophilicity. Considering the
657 oxygen barrier property, CHI, LMP, KC, SA, CS and PL films displayed good oxygen barrier
658 properties in semi-dry (50 % RH) and humid (80 % RH) conditions. Among all polysaccha-
659 rides, SA even presented the highest oxygen barrier, with permeance values comparable to
660 those of conventional high oxygen barrier plastics, such as EVOH and PVDC. On the contra-
661 ry, cellulose derivatives (HPMC, MC and HPC) showed low oxygen barrier performance
662 both in semi-dry and humid conditions. The implementation of polysaccharides for packaging
663 applications represents an opportunity for waste valorization, contributing to the concept of a
664 circular economy. The most promising application of polysaccharides could be their use as
665 coating materials on paper-based packaging, offering a good protective barrier against oxy-
666 gen for oxidation-sensitive food products. They might also help in the strategies to replace
667 conventional coating materials, which are based on synthetic polymers, leading to recyclabil-
668 ity issues for such multilayer materials.

669 **Declaration of competing interest**

670 The authors have declared no conflict of interest.

671 **Credit authorship contribution statement**

672 **María Ureña:** Conceptualization, Methodology, Formal analysis, Investigation, Writing –
673 original draft. **Thị- Thanh-Trúc Phùng:** Conceptualization, Methodology, Writing – review
674 & editing. **Massimiliano Gerometta:** Methodology, Writing – review & editing. **Luciana de**
675 **Siqueira Oliveira:** Methodology, Writing – review & editing. **Julie Chanut:** Methodology,
676 Writing – review & editing. **Sandra Domenek:** Methodology, Writing – review & editing.
677 **Patrice Dole:** Methodology, Writing – review & editing. **Gaelle Roudaut:** Methodology,
678 Writing – review & editing. **Aurélie Lagorce:** Conceptualization, Methodology, Writing –
679 review & editing. **Thomas Karbowski:** Conceptualization, Methodology, Formal analysis,
680 Investigation, Writing – original draft.

681 **Acknowledgment**

682 This work was supported by the Carnot Qualiment, the DIVVA (Développement Innovation
683 Vigne Vin Aliments) platform, the Regional Council of Bourgogne Franche Comté and the
684 "Fonds Européen de Développement Régional (FEDER)". We also thank Thuy Linh Nguyen,
685 Bernadette Rollin and Adrien Lebreton for technical support as well as Antoine Rouilly for
686 valuable discussion.

687 **References**

- 688 Abdan, K. B., Yong, S. C., Chiang, E. C. W., Talib, R. A., Hui, T. C., & Hao, L. C. (2020). Barrier
689 properties, antimicrobial and antifungal activities of chitin and chitosan-based IPNs, gels,
690 blends, composites, and nanocomposites. In *Handbook of Chitin and Chitosan* (pp. 175–227).
691 Elsevier. <https://doi.org/10.1016/B978-0-12-817968-0.00006-8>
- 692 Avella, M., Pace, E. D., Immirzi, B., Impallomeni, G., Malinconico, M., & Santagata, G. (2007). Ad-
693 dition of glycerol plasticizer to seaweeds derived alginates: Influence of microstructure on
694 chemical–physical properties. *Carbohydrate Polymers*, *69*(3), 503–511.
695 <https://doi.org/10.1016/j.carbpol.2007.01.011>
- 696 Chen, Y.-H., Cheng, C.-C., & Lee, D.-J. (2021). Synthesis of low surface energy thin films of nonhal-
697 ogenated polyepichlorohydrin-triazoles with side alkyl chain. *Surfaces and Interfaces*, *24*,
698 101153. <https://doi.org/10.1016/j.surfin.2021.101153>
- 699 Choi, S.-G., Kim, K. M., Hanna, M. A., Weller, C. L., & Kerr, W. L. (2003). Molecular Dynamics of
700 Soy-Protein Isolate Films Plasticized by Water and Glycerol. *Journal of Food Science*, *68*(8),
701 2516–2522. <https://doi.org/10.1111/j.1365-2621.2003.tb07054.x>

702 Crouvisier-Urien, K., Bodart, P. R., Winckler, P., Raya, J., Gougeon, R. D., Cayot, P., Domenek, S.,
703 Debeaufort, F., & Karbowski, T. (2016). Biobased Composite Films from Chitosan and Lignin:
704 Antioxidant Activity Related to Structure and Moisture. *ACS Sustainable Chemistry & Engi-*
705 *neering*, 4(12), 6371–6381. <https://doi.org/10.1021/acssuschemeng.6b00956>

706 Deshwal, G. K., Panjagari, N. R., & Alam, T. (2019). An overview of paper and paper-based food
707 packaging materials: Health safety and environmental concerns. *Journal of Food Science and*
708 *Technology*, 56(10), 4391–4403. <https://doi.org/10.1007/s13197-019-03950-z>

709 Edens, R. E. (2005). Polysaccharides: Structural Diversity and Functional Versatility. *Journal of the*
710 *American Chemical Society*, 127(28), 10119–10119. <https://doi.org/10.1021/ja0410486>

711 Elidrissi, A. (2012). New approach to predict the solubility of polymers Application: Cellulose Ace-
712 tate at various DS, prepared from Alfa “Stipa—Tenassicima” of Eastern Morocco. *Journal of*
713 *Materials and Environmental Science*, 122(5), 2952–2965. <https://doi.org/10.1002/app.34028>

714 Espinoza-Herrera, N., Pedroza-Islas, R., San Martín-Martinez, E., Cruz-Orea, A., & Tomás, S. A.
715 (2011). Thermal, Mechanical and Microstructures Properties of Cellulose Derivatives Films: A
716 Comparative Study. *Food Biophysics*, 6(1), 106–114. <https://doi.org/10.1007/s11483-010-9181-0>

717 European Parliament and Council Directive 94/62/EC. (2018). *European Parliament and Council*
718 *Directive 94/62/EC*. <https://www.legislation.gov.uk/eudr/1994/62/contents>

719 Fathi Azarbayjani, A., Jouyban, A., & Chan, S. Y. (2009). Impact of Surface Tension in Pharmaceuti-
720 cal Sciences. *Journal of Pharmacy & Pharmaceutical Sciences*, 12(2), 218.
721 <https://doi.org/10.18433/J32P40>

722 Fluidan. (2018). *Automate viscosity control in manufacture of paint*.
723 <https://fluidan.com/manufacturing-of-paint/>

724 Guo, Q., Liu, Y., & Cui, S. W. (2021). Structure, classification and modification of polysaccharides. In
725 *Comprehensive Glycoscience* (pp. 204–229). Elsevier. [https://doi.org/10.1016/B978-0-12-](https://doi.org/10.1016/B978-0-12-819475-1.00094-8)
726 [819475-1.00094-8](https://doi.org/10.1016/B978-0-12-819475-1.00094-8)

727 Hansen, C. M. (2007). *Hansen solubility parameters: A user’s handbook* (2nd ed.). CRC Press.
728 [https://www.routledge.com/Hansen-Solubility-Parameters-A-Users-Handbook-Second-](https://www.routledge.com/Hansen-Solubility-Parameters-A-Users-Handbook-Second-Edition/Hansen/p/book/9780849372483)
729 [Edition/Hansen/p/book/9780849372483](https://www.routledge.com/Hansen-Solubility-Parameters-A-Users-Handbook-Second-Edition/Hansen/p/book/9780849372483)

730 Hosseini, S. F., Ghaderi, J., & Gómez-Guillén, M. C. (2020). trans-Cinnamaldehyde-doped quadripar-
731 tite biopolymeric films: Rheological behavior of film-forming solutions and biofunctional per-
732 formance of films. *Food Hydrocolloids*, 112, 106339.
733 <https://doi.org/10.1016/j.foodhyd.2020.106339>

- 734 Immergut, E., H., & Mark, H. F. (1965). Principles of Plasticization. In N. A. J. Platzer (Ed.), *Plastici-*
735 *zation and plasticizer processes* (Vol. 48, pp. 1–26). American Chemical Society.
736 <https://doi.org/10.1021/ba-1965-0048>
- 737 International Organization for Standardization. (2017). *ISO 2528:2017 Sheet materials—*
738 *Determination of water vapour transmission rate (WVTR)—Gravimetric (dish) method.*
739 <https://www.iso.org/standard/72382.html>
- 740 International Organization for Standardization. (2018). *ISO 527-3:2018 Plastics—Determination of*
741 *tensile properties—Part 3: Test conditions for films and sheets.*
742 <https://www.iso.org/standard/70307.html>
- 743 Jantrawut, P., Chaiwarit, T., Jantanasakulwong, K., Brachais, C., & Chambin, O. (2017). Effect of
744 plasticizer type on tensile property and In Vitro indomethacin release of thin films based on low-
745 methoxyl pectin. *Polymers*, 9(12), 289. <https://doi.org/10.3390/polym9070289>
- 746 Jarray, A., Gerbaud, V., & Hemati, M. (2016). Polymer-plasticizer compatibility during coating for-
747 mulation: A multi-scale investigation. *Progress in Organic Coatings*, 101, 195–206.
748 <https://doi.org/10.1016/j.porgcoat.2016.08.008>
- 749 Kchaou, H., Jridi, M., Benbettaieb, N., Debeaufort, F., & Nasri, M. (2020). Bioactive films based on
750 cuttlefish (*Sepia officinalis*) skin gelatin incorporated with cuttlefish protein hydrolysates: Phys-
751 icochemical characterization and antioxidant properties. *Food Packaging and Shelf Life*, 24,
752 100477. <https://doi.org/10.1016/j.fpsl.2020.100477>
- 753 Khalil, H. P. S. A., Saurabh, C. K., Syakir, M. I., Fazita, M. R. N., Bhat, A., Banerjee, A., Fizree, H.
754 M., Rizal, S., & Tahir, P. M. (2019). Barrier properties of biocomposites/hybrid films. In M. Ja-
755 waid, M. Thariq, & N. Saba (Eds.), *Mechanical and Physical Testing of Biocomposites, Fibre-*
756 *Reinforced Composites and Hybrid Composites* (pp. 241–258). Woodhead Publishing.
757 <https://doi.org/10.1016/B978-0-08-102292-4.00013-8>
- 758 Krevelen, D. W., & Nijenhuis, K. te. (2009). *Properties of polymers: Their correlation with chemical*
759 *structure their numerical estimation and prediction from additive group contributions* (4th ed.).
760 Elsevier. <https://www.sciencedirect.com/book/9780080548197/properties-of-polymers>
- 761 Lagaron, J. M., Catalá, R., & Gavara, R. (2004). Structural characteristics defining high barrier prop-
762 erties in polymeric materials. *Materials Science and Technology*, 20(1), 1–7.
763 <https://doi.org/10.1179/026708304225010442>

- 764 Ma, J., Lin, Y., Chen, X., Zhao, B., & Zhang, J. (2014). Flow behavior, thixotropy and dynamical
765 viscoelasticity of sodium alginate aqueous solutions. *Food Hydrocolloids*, 38, 119–128.
766 <https://doi.org/10.1016/j.foodhyd.2013.11.016>
- 767 Madeleine-Perdrillat, C., Karbowiak, T., Debeaufort, F., Delmotte, L., Vaultot, C., & Champion, D.
768 (2016). Effect of hydration on molecular dynamics and structure in chitosan films. *Food Hydro-*
769 *colloids*, 61, 57–65. <https://doi.org/10.1016/j.foodhyd.2016.04.035>
- 770 Monte, M. L., Moreno, M. L., Senna, J., Arrieche, L. S., & Pinto, L. A. A. (2018). Moisture sorption
771 isotherms of chitosan-glycerol films: Thermodynamic properties and microstructure. *Food Bio-*
772 *science*, 22, 170–177. <https://doi.org/10.1016/j.fbio.2018.02.004>
- 773 Nasatto, P., Pignon, F., Silveira, J., Duarte, M., Nosedá, M., & Rinaudo, M. (2015). Methylcellulose, a
774 Cellulose Derivative with Original Physical Properties and Extended Applications. *Polymers*,
775 7(5), 777–803. <https://doi.org/10.3390/polym7050777>
- 776 Nechita, P., & Roman, M. (2020). Review on polysaccharides used in coatings for food packaging
777 papers. *Coatings*, 10(6), 566. <https://doi.org/10.3390/coatings10060566>
- 778 Pamies, R., Schmidt, R. R., Martínez, M. del C. L., & De la Torre, J. G. (2010). The influence of
779 mono and divalent cations on dilute and non-dilute aqueous solutions of sodium alginates. *Car-*
780 *bohydrate Polymers*, 80(1), 248–253. <https://doi.org/10.1016/j.carbpol.2009.11.020>
- 781 Parker, L. (2019). *The world's plastic pollution crisis explained*.
782 <https://www.nationalgeographic.com/environment/article/plastic-pollution>
- 783 Salem, A., Jridi, M., Abdelhedi, O., Fakhfakh, N., Nasri, M., Debeaufort, F., & Zouari, N. (2021).
784 Development and characterization of fish gelatin-based biodegradable film enriched with Lepid-
785 ium sativum extract as active packaging for cheese preservation. *Heliyon*, 7(10), e08099.
786 <https://doi.org/10.1016/j.heliyon.2021.e08099>
- 787 Saraiva, M., Gamelas, J. A., Mendes de Sousa, A., Reis, B., Amaral, J., & Ferreira, P. (2010). A New
788 Approach for the Modification of Paper Surface Properties Using Polyoxometalates. *Materials*,
789 3(1), 201–215. <https://doi.org/10.3390/ma3010201>
- 790 Shankar, S., Tanomrod, N., Rawdkuen, S., & Rhim, J.-W. (2016). Preparation of pectin/silver nano-
791 particles composite films with UV-light barrier and properties. *International Journal of Biologi-*
792 *cal Macromolecules*, 92, 842–849. <https://doi.org/10.1016/j.ijbiomac.2016.07.107>
- 793 Sharmin, N., Sone, I., Walsh, J. L., Sivertsvik, M., & Fernández, E. N. (2021). Effect of citric acid and
794 plasma activated water on the functional properties of sodium alginate for potential food packag-

795 ing applications. *Food Packaging and Shelf Life*, 29, 100733.
796 <https://doi.org/10.1016/j.fpsl.2021.100733>

797 Smith, D. R., Escobar, A. P., Andris, M. N., Boardman, B. M., & Peters, G. M. (2021). Understanding
798 the Molecular-Level Interactions of Glucosamine-Glycerol Assemblies: A Model System for
799 Chitosan Plasticization. *ACS Omega*, 6(39), 25227–25234.
800 <https://doi.org/10.1021/acsomega.1c03016>

801 Sothornvit, R., & Krochta, J. M. (2005). Plasticizers in edible films and coatings. In *Innovations in*
802 *Food Packaging* (pp. 403–433). Elsevier. <https://doi.org/10.1016/B978-012311632-1/50055-3>

803 Stoica, M., Marian Antohi, V., Laura Zlati, M., & Stoica, D. (2020). The financial impact of replacing
804 plastic packaging by biodegradable biopolymers—A smart solution for the food industry. *Jour-*
805 *nal of Cleaner Production*, 277, 124013. <https://doi.org/10.1016/j.jclepro.2020.124013>

806 Su, J.-F., Huang, Z., Zhao, Y.-H., Yuan, X.-Y., Wang, X.-Y., & Li, M. (2010). Moisture sorption and
807 water vapor permeability of soy protein isolate/poly(vinyl alcohol)/glycerol blend films. *Indus-*
808 *trial Crops and Products*, 31(2), 266–276. <https://doi.org/10.1016/j.indcrop.2009.11.010>

809 Sun Lee, D., L.Yam, K., & PierGiovanni, L. (2008). *Food packaging science and technology* (2nd
810 ed). Taylor & Francis Group. . <https://books.google.fr/books?id=DpnMuQEACAAJ>

811 Tardy, B. L., Richardson, J. J., Greca, L. G., Guo, J., Bras, J., & Rojas, O. J. (2022). Advancing bio-
812 based materials for sustainable solutions to food packaging. *Nature Sustainability*, 6(360–367).
813 <https://doi.org/10.1038/s41893-022-01012-5>

814 Udayakumar, M., Kollár, M., Kristály, F., Leskó, M., Szabó, T., Marossy, K., Tasnádi, I., & Németh,
815 Z. (2020). Temperature and Time Dependence of the Solvent-Induced Crystallization of Poly(l-
816 lactide). *Polymers*, 12(5), 1065. <https://doi.org/10.3390/polym12051065>

817 United Nations Environment Programme. (2018). *Single-use plastics, a roadmap for sustainability*.
818 <https://www.unep.org/resources/report/single-use-plastics-roadmap-sustainability>

819 Venelampi, O., Weber, A., Rönkkö, T., & Itävaara, M. (2003). The Biodegradation and Disintegration
820 of Paper Products in the Composting Environment. *Compost Science & Utilization*, 11(3), 200–
821 209. <https://doi.org/10.1080/1065657X.2003.10702128>

822 Wang, J., Gardner, D. J., Stark, N. M., Bousfield, D. W., Tajvidi, M., & Cai, Z. (2018). Moisture and
823 oxygen barrier properties of cellulose nanomaterial-based films. *ACS Sustainable Chemistry &*
824 *Engineering*, 6(1), 49–70. <https://doi.org/10.1021/acssuschemeng.7b03523>

- 825 Wu, F., Misra, M., & Mohanty, A. K. (2021). Challenges and new opportunities on barrier perfor-
826 mance of biodegradable polymers for sustainable packaging. *Progress in Polymer Science*, *117*,
827 101395. <https://doi.org/10.1016/j.progpolymsci.2021.101395>
- 828 Xiao, Q., & Tong, Q. (2013). Thermodynamic properties of moisture sorption in pullulan–sodium
829 alginate based edible films. *Food Research International*, *54*(2), 1605–1612.
830 <https://doi.org/10.1016/j.foodres.2013.09.019>
- 831 Xu, Y., Han, Y., Chen, M., Li, J., Li, J., Luo, J., & Gao, Q. (2022). A soy protein-based film by mixed
832 covalent cross-linking and flexibilizing networks. *Industrial Crops and Products*, *183*, 114952.
833 <https://doi.org/10.1016/j.indcrop.2022.114952>
- 834 Yadav, H., & Karthikeyan, C. (2019). Natural polysaccharides: Structural features and properties. In
835 *Polysaccharide Carriers for Drug Delivery* (pp. 1–17). Elsevier. <https://doi.org/10.1016/B978-0->
836 [08-102553-6.00001-5](https://doi.org/10.1016/B978-0-08-102553-6.00001-5)
- 837 Younis, H. G. R., Abdellatif, H. R. S., Ye, F., & Zhao, G. (2020). Tuning the physicochemical proper-
838 ties of apple pectin films by incorporating chitosan/pectin fiber. *International Journal of Biolog-*
839 *ical Macromolecules*, *159*, 213–221. <https://doi.org/10.1016/j.ijbiomac.2020.05.060>
- 840 Yousif, E., & Haddad, R. (2013). Photodegradation and photostabilization of polymers, especially
841 polystyrene: Review. *SpringerPlus*, *2*(1), 398. <https://doi.org/10.1186/2193-1801-2-398>

842 APPENDIX A. Barrier properties of polysaccharide films to water vapor and oxygen. **HPMC**: Hydroxypropyl Methylcellulose. **MC**: Methyl Cellulose. **HPC**: Hydroxypropyl
843 Cellulose. **LMP**: Low Methoxyl Pectin. **CS**: Cationic Starch. **SA**: Sodium Alginate. **KC**: Kappa-Carrageenan. **CHI**: Chitosan. **PL**: Pullulan. **RH**: relative humidity. **N/A**: not

Polysaccharide	% glycerol	Water vapor permeance (mol.m ⁻² .s ⁻¹ .Pa ⁻¹)		Oxygen permeance (mol.m ⁻² .s ⁻¹ .Pa ⁻¹)		
		0-50 % RH	50-100 % RH	10 % RH	50 % RH	80 % RH
HPMC	0	6.96x10 ⁻⁸ ±6.78x10 ⁻⁹ ^α	1.66x10 ⁻⁷ ±6.85x10 ⁻⁹ ^{αβ}	5.43x10 ⁻¹² ±7.06x10 ⁻¹³ ^α	2.85x10 ⁻¹² ±5.19x10 ⁻¹³ ^α	2.77x10 ⁻¹² ±2.99x10 ⁻¹³ ^α
	10	8.28x10 ⁻⁸ ±6.39x10 ⁻⁹ ^{αβ}	1.94x10 ⁻⁷ ±4.88x10 ⁻⁹ ^α	1.84x10 ⁻¹² ±1.11x10 ⁻¹³ ^β	1.94x10 ⁻¹² ±3.95x10 ⁻¹³ ^β	2.20x10 ⁻¹² ±4.61x10 ⁻¹³ ^{αβ}
	20	1.08x10 ⁻⁷ ±1.17x10 ⁻⁸ ^{βδ}	2.24x10 ⁻⁷ ±5.67x10 ⁻⁹ ^{αβ}	1.38x10 ⁻¹² ±5.50x10 ⁻¹⁴ ^δ	1.86x10 ⁻¹² ±4.35x10 ⁻¹⁴ ^β	1.98x10 ⁻¹² ±1.72x10 ⁻¹³ ^β
	30	1.08x10 ⁻⁷ ±1.07x10 ⁻⁸ ^δ	2.68x10 ⁻⁷ ±3.33x10 ⁻⁹ ^β	1.31x10 ⁻¹² ±9.53x10 ⁻¹⁴ ^δ	2.35x10 ⁻¹² ±1.74x10 ⁻¹³ ^{αβ}	2.47x10 ⁻¹² ±1.60x10 ⁻¹³ ^{αβ}
MC	0	9.10x10 ⁻⁸ ±2.87x10 ⁻⁸ ^α	1.86x10 ⁻⁷ ±4.14x10 ⁻⁹ ^α	2.74x10 ⁻¹² ±8.09x10 ⁻¹³ ^α	1.40x10 ⁻¹² ±1.11x10 ⁻¹³ ^α	1.63x10 ⁻¹² ±2.38x10 ⁻¹³ ^α
	10	1.05x10 ⁻⁷ ±1.27x10 ⁻⁸ ^α	2.21x10 ⁻⁷ ±1.03x10 ⁻⁹ ^β	8.61x10 ⁻¹³ ±3.66x10 ⁻¹⁴ ^β	1.14x10 ⁻¹² ±1.15x10 ⁻¹³ ^β	1.45x10 ⁻¹² ±3.16x10 ⁻¹³ ^α
	20	7.39x10 ⁻⁸ ±2.27x10 ⁻⁹ ^α	2.52x10 ⁻⁷ ±4.81x10 ⁻⁹ ^δ	6.62x10 ⁻¹³ ±2.43x10 ⁻¹⁴ ^β	1.22x10 ⁻¹² ±6.55x10 ⁻¹⁴ ^{αβ}	1.36x10 ⁻¹² ±2.08x10 ⁻¹⁴ ^α
	30	1.26x10 ⁻⁷ ±9.03x10 ⁻⁹ ^α	2.75x10 ⁻⁷ ±6.61x10 ⁻⁹ ^ψ	5.75x10 ⁻¹³ ±2.90x10 ⁻¹⁴ ^β	1.09x10 ⁻¹² ±7.09x10 ⁻¹⁴ ^β	1.30x10 ⁻¹² ±1.05x10 ⁻¹³ ^α
HPC	0	4.84x10 ⁻⁸ ±9.84x10 ⁻¹⁰	1.27x10 ⁻⁷ ±4.16x10 ⁻⁹	1.49x10 ⁻¹² ±8.50x10 ⁻¹⁴	1.83x10 ⁻¹² ±2.10x10 ⁻¹³	2.11x10 ⁻¹² ±1.21x10 ⁻¹³
	10	5.23x10 ⁻⁸ ±2.42x10 ⁻⁹	1.94x10 ⁻⁷ ±4.82x10 ⁻⁹	1.71x10 ⁻¹² ±3.61x10 ⁻¹³	2.34x10 ⁻¹² ±4.12x10 ⁻¹³	2.80x10 ⁻¹² ±5.60x10 ⁻¹³
LMP	20	5.60x10 ⁻⁸ ±6.56x10 ⁻⁹	2.33x10 ⁻⁷ ±7.87x10 ⁻⁹	N/A	2.33x10 ⁻¹⁴ ±8.53x10 ⁻¹⁵	7.57x10 ⁻¹³ ±9.60x10 ⁻¹⁴
	30	7.56x10 ⁻⁸ ±2.72x10 ⁻⁹	2.60x10 ⁻⁷ ±8.08x10 ⁻⁹	N/A	3.76x10 ⁻¹⁴ ±2.00x10 ⁻¹⁵	1.10x10 ⁻¹² ±2.84x10 ⁻¹³
CS	0	5.38x10 ⁻⁸ ±8.80x10 ⁻⁹ ^α	2.27x10 ⁻⁷ ±9.29x10 ⁻⁹ ^β	N/A	N/A	N/A
	10	3.85x10 ⁻⁸ ±3.19x10 ⁻⁹ ^β	1.87x10 ⁻⁷ ±1.48x10 ⁻⁸ ^α	N/A	3.12x10 ⁻¹⁴ ±4.08x10 ⁻¹⁴ ^α	7.78x10 ⁻¹⁴ ±4.03x10 ⁻¹⁴
	20	4.38x10 ⁻⁸ ±5.27x10 ⁻⁹ ^β	2.39x10 ⁻⁷ ±1.26x10 ⁻⁸ ^β	N/A	1.28x10 ⁻¹⁴ ±3.33x10 ⁻¹⁵ ^α	8.91x10 ⁻¹⁴ ±3.65x10 ⁻¹⁵
	30	5.39x10 ⁻⁸ ±1.67x10 ⁻⁹ ^β	2.87x10 ⁻⁷ ±1.47x10 ⁻⁸ ^δ	N/A	3.61x10 ⁻¹⁴ ±1.72x10 ⁻¹⁴ ^α	N/A
SA	0	9.22x10 ⁻⁸ ±4.37x10 ⁻⁹ ^α	3.53x10 ⁻⁷ ±1.79x10 ⁻⁸ ^α	N/A	5.40x10 ⁻¹⁵ ±3.40x10 ⁻¹⁵ ^α	6.88x10 ⁻¹⁴ ±1.51x10 ⁻¹⁴ ^α
	10	6.52x10 ⁻⁸ ±4.84x10 ⁻⁹ ^α	2.67x10 ⁻⁷ ±1.28x10 ⁻⁸ ^β	N/A	2.63x10 ⁻¹⁵ ±1.39x10 ⁻¹⁵ ^α	1.73x10 ⁻¹³ ±1.93x10 ⁻¹³ ^β
	20	9.20x10 ⁻⁸ ±7.97x10 ⁻⁹ ^α	2.66x10 ⁻⁷ ±1.84x10 ⁻⁸ ^β	N/A	3.24x10 ⁻¹⁵ ±2.52x10 ⁻¹⁵ ^β	1.97x10 ⁻¹³ ±8.71x10 ⁻¹⁵ ^{αβ}
	30	7.32x10 ⁻⁸ ±1.01x10 ⁻⁸ ^α	2.77x10 ⁻⁷ ±1.34x10 ⁻⁸ ^β	N/A	8.19x10 ⁻¹⁵ ±3.51x10 ⁻¹⁵ ^α	5.33x10 ⁻¹³ ±2.23x10 ⁻¹³ ^{αβ}
KC	10	1.00x10 ⁻⁷ ±8.91x10 ⁻¹⁰ ^α	3.00x10 ⁻⁷ ±8.82x10 ⁻⁹ ^α	N/A	9.41x10 ⁻¹⁵ ±5.43x10 ⁻¹⁵ ^α	7.26x10 ⁻¹³ ±3.28x10 ⁻¹³ ^α
	20	1.01x10 ⁻⁷ ±6.44x10 ⁻⁹ ^β	3.10x10 ⁻⁷ ±1.82x10 ⁻⁸ ^α	N/A	1.32x10 ⁻¹⁴ ±1.44x10 ⁻¹⁵ ^α	7.95x10 ⁻¹³ ±2.18x10 ⁻¹³ ^α
	30	1.06x10 ⁻⁷ ±3.80x10 ⁻⁹ ^δ	3.37x10 ⁻⁷ ±5.47x10 ⁻⁹ ^β	N/A	4.53x10 ⁻¹⁴ ±2.04x10 ⁻¹⁵ ^α	1.38x10 ⁻¹² ±6.35x10 ⁻¹⁴ ^β
CHI	0	1.68x10 ⁻⁸ ±1.09x10 ⁻⁹ ^α	1.72x10 ⁻⁷ ±2.14x10 ⁻⁸ ^α	N/A	9.49x10 ⁻¹⁵ ±2.27x10 ⁻¹⁵ ^α	N/A
	10	2.16x10 ⁻⁸ ±6.11x10 ⁻¹⁰ ^α	2.06x10 ⁻⁷ ±6.06x10 ⁻⁹ ^{αβ}	N/A	3.20x10 ⁻¹⁴ ±1.33x10 ⁻¹⁴ ^{αβ}	N/A
	20	4.60x10 ⁻⁸ ±1.00x10 ⁻⁸ ^β	2.18x10 ⁻⁷ ±1.35x10 ⁻⁸ ^{αβ}	N/A	2.90x10 ⁻¹⁴ ±9.89x10 ⁻¹⁵ ^{αβ}	N/A
	30	6.93x10 ⁻⁸ ±6.64x10 ⁻⁹ ^δ	2.52x10 ⁻⁷ ±9.32x10 ⁻⁹ ^β	N/A	3.73x10 ⁻¹⁴ ±4.26x10 ⁻¹⁵ ^β	N/A
PL	0	5.12x10 ⁻⁸ ±5.95x10 ⁻⁹ ^α	2.47x10 ⁻⁷ ±2.28x10 ⁻⁸ ^α	N/A	2.32x10 ⁻¹⁴ ±5.5x10 ⁻¹⁶ ^α	N/A
	10	2.58x10 ⁻⁸ ±2.04x10 ⁻⁹ ^β	1.61x10 ⁻⁷ ±1.05x10 ⁻⁸ ^β	N/A	2.46x10 ⁻¹⁴ ±1.39x10 ⁻¹⁶ ^α	N/A
	20	3.36x10 ⁻⁸ ±6.29x10 ⁻⁹ ^β	2.16x10 ⁻⁷ ±1.47x10 ⁻⁹ ^α	N/A	1.18x10 ⁻¹⁴ ±6.74x10 ⁻¹⁵ ^α	N/A

844 applicable.

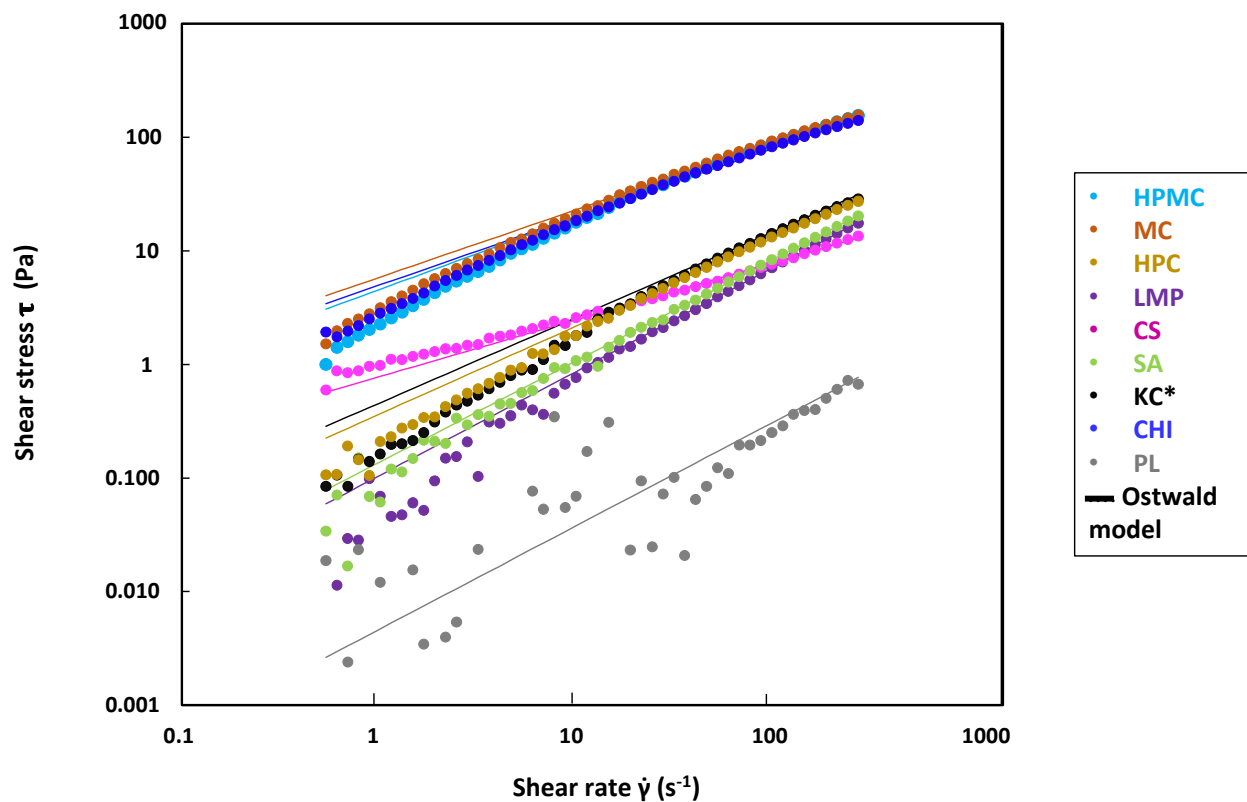
845 Values are reported as mean \pm standard deviation. Significant differences with a p-value < 0.05 are provided. The characters α , β , δ , ψ are used to identify the difference of a parameter for the same polymer with different
 846 glycerol ratios.

847 **APPENDIX B.** Mechanical properties of polysaccharide films. **HPMC:** Hydroxypropyl Methylcellulose. **MC:** Methyl Cellulose. **HPC:** Hydroxypropyl Cellulose. **LMP:** Low
 848 Methoxyl Pectin. **CS:** Cationic Starch. **SA:** Sodium Alginate. **KC:** Kappa-Carrageenan. **CHI:** Chitosan. **PL:** Pullulan.






Polysaccharide	% glycerol	Young's modulus (GPa)	Tensile strength (MPa)	Elongation at break (%)
HPMC	0	2.72 \pm 0.18 $^{\alpha}$	60.11 \pm 29.16 $^{\alpha}$	5.62 \pm 4.51 $^{\alpha}$
	10	2.09 \pm 0.10 $^{\beta}$	68.48 \pm 11.63 $^{\alpha}$	18.55 \pm 6.43 $^{\beta}$
	20	1.57 \pm 0.04 $^{\delta}$	69.48 \pm 7.25 $^{\alpha}$	33.62 \pm 3.86 $^{\delta}$
	30	1.24 \pm 0.03 $^{\psi}$	52.36 \pm 4.58 $^{\alpha}$	36.85 \pm 4.53 $^{\delta}$
MC	0	2.72 \pm 0.20 $^{\alpha}$	79.35 \pm 16.41 $^{\alpha}$	11.04 \pm 6.84 $^{\alpha}$
	10	2.23 \pm 0.16 $^{\beta}$	59.63 \pm 15.66 $^{\beta}$	14.50 \pm 10.69 $^{\alpha}$
	20	1.54 \pm 0.10 $^{\delta}$	51.14 \pm 4.60 $^{\beta}$	28.50 \pm 4.82 $^{\beta}$
	30	1.23 \pm 0.11 $^{\psi}$	50.30 \pm 6.84 $^{\beta}$	37.50 \pm 4.90 $^{\beta}$
HPC	0	0.51 \pm 0.05	14.14 \pm 2.86	65.64 \pm 33.78
	10	0.17 \pm 0.08	11.69 \pm 3.00	123.28 \pm 16.56
LMP	20	4.28 \pm 0.19	92.37 \pm 10.95	3.08 \pm 1.12
	30	3.35 \pm 0.17	74.99 \pm 9.45	4.41 \pm 2.10
CS	0	2.59 \pm 0.13 $^{\alpha}$	49.19 \pm 5.19 $^{\alpha}$	4.38 \pm 2.24 $^{\alpha}$
	10	2.16 \pm 0.04 $^{\beta}$	45.53 \pm 5.95 $^{\alpha}$	3.06 \pm 1.00 $^{\alpha}$
	20	1.50 \pm 0.15 $^{\delta}$	30.55 \pm 6.84 $^{\beta}$	2.93 \pm 0.85 $^{\alpha}$
	30	0.80 \pm 0.19 $^{\psi}$	16.25 \pm 3.54 $^{\delta}$	3.33 \pm 0.69 $^{\alpha}$
SA	0	5.46 \pm 0.53 $^{\alpha}$	86.37 \pm 11.66 $^{\alpha}$	3.49 \pm 1.65 $^{\alpha}$
	10	4.24 \pm 0.67 $^{\beta}$	84.66 \pm 9.58 $^{\alpha\beta}$	5.12 \pm 2.05 $^{\alpha}$
	20	3.21 \pm 0.58 $^{\delta}$	65.13 \pm 22.46 $^{\beta\delta}$	7.19 \pm 5.55 $^{\alpha}$
	30	2.40 \pm 0.24 $^{\psi}$	52.74 \pm 7.36 $^{\delta}$	8.30 \pm 4.37 $^{\alpha}$
KC	10	3.38 \pm 0.35 $^{\alpha}$	68.10 \pm 28.47 $^{\alpha}$	2.75 \pm 1.30 $^{\alpha}$
	20	2.72 \pm 0.34 $^{\beta}$	15.61 \pm 8.16 $^{\beta}$	0.55 \pm 0.41 $^{\beta}$
	30	2.28 \pm 0.33 $^{\beta}$	36.36 \pm 16.04 $^{\beta}$	1.77 \pm 0.96 $^{\beta}$
CHI	0	4.06 \pm 0.34 $^{\alpha}$	104.18 \pm 9.62 $^{\alpha}$	3.22 \pm 0.79 $^{\alpha}$
	10	2.53 \pm 0.19 $^{\beta}$	74.17 \pm 4.61 $^{\beta}$	4.51 \pm 0.73 $^{\beta}$
	20	2.33 \pm 0.16 $^{\beta}$	59.8 \pm 11.49 $^{\delta}$	3.83 \pm 1.25 $^{\beta}$
	30	1.44 \pm 0.13 $^{\delta}$	38.21 \pm 3.58 $^{\psi}$	9.08 \pm 6.73 $^{\delta}$
PL	0	2.87 \pm 0.24 $^{\alpha}$	50.77 \pm 7.25 $^{\alpha}$	2.64 \pm 0.48 $^{\alpha}$
	10	2.70 \pm 0.28 $^{\alpha}$	49.77 \pm 5.97 $^{\alpha}$	2.37 \pm 0.30 $^{\alpha}$
	20	1.76 \pm 0.27 $^{\beta}$	30.01 \pm 2.99 $^{\beta}$	2.18 \pm 0.37 $^{\alpha}$

849 Values are reported as mean \pm standard deviation. Significant differences with a p-value < 0.05 are provided. The characters α , β , δ , ψ are used to identify the difference of a parameter for the same polymer with differ-
 850 ent glycerol ratio.

851
852
853



Appendix C. Shear stress (τ) as a function of shear rate ($\dot{\gamma}$) of polysaccharide solutions measured at $25(\pm 1)$ °C. Continuous lines represent the fitted curves based on the Ostwald de Waele model. **HPMC:** Hydroxypropyl Methylcellulose. **MC:** Methyl Cellulose. **HPC:** Hydroxypropyl Cellulose. **LMP:** Low Methoxyl Pectin. **CS:** Cationic Starch. **SA:** Sodium Alginate. **KC:** Kappa-Carrageenan (*: Temperature of measurement $70(\pm 1)$ °C). **CHI:** Chitosan. **PL:** Pullulan.

Polysaccharides	
Cellulose derivatives	
Pectin	
Starch	
Alginate	
Carrageenan	
Chitosan	